REVIEW

Solid-State Batteries

Solid-State Sodium Batteries

Chenglong Zhao, Lilu Liu, Xingguo Qi, Yaxiang Lu,* Feixiang Wu, Junmei Zhao, Yan Yu,* Yong-Sheng Hu,* and Liquan Chen

Rechargeable Na-ion batteries (NIBs) are attractive large-scale energy storage systems compared to Li-ion batteries due to the substantial reserve and low cost of sodium resources. The recent rapid development of NIBs will no doubt accelerate the commercialization process. As one of the indispensable components in current battery systems, organic liquid electrolytes are widely used for their high ionic conductivity and good wettability, but the low thermal stability, especially the easy flammability and leakage make them at risk of safety issues. The booming solid-state batteries with solid-state electrolytes (SSEs) show promise as alternatives to organic liquid systems due to their improved safety and higher energy density. However, several challenges including low ionic conductivity, poor wettability, low stability/incompatibility between electrodes and electrolytes, etc., may degrade performance, hindering the development of practical applications. In this review, an overview of Na-ion SSEs is first outlined according to the classification of solid polymer electrolytes, composite polymer electrolytes, inorganic solid electrolytes, etc. Furthermore, the current challenges and critical perspectives for the potential development of solid-state sodium batteries are discussed in detail.

C. Zhao, L. Liu, X. Qi, Dr. Y. Lu, Prof. Y.-S. Hu, Prof. L. Chen
Key Laboratory for Renewable Energy
Beijing Key Laboratory for New Energy Materials and Devices
Beijing National Laboratory for Condensed Matter Physics
Institute of Physics
Chinese Academy of Sciences
School of Physical Sciences
University of Chinese Academy of Sciences
Beijing 100190, China
E-mail: yxlu@iphy.ac.cn; yshu@aphy.iphy.ac.cn
Dr. F. Wu, Prof. Y. Yu
Max Planck Institute for Solid State Research Heisenbergstr. 1
Stuttgart 70569, Germany
Prof. J. Zhao
Key Laboratory of Green Process and Engineering
Institute of Process Engineering
Chinese Academy of Sciences
Beijing 100190, China
Prof. Y. Yu
Key Laboratory of Materials for Energy Conversion
Chinese Academy of Sciences
Department of Materials Science and Engineering
University of Science and Technology of China
Hefei, Anhui 230026, China
E-mail: yanyumse@ustc.edu.cn

The ORCID identification number(s) for the author(s) of this article can be found under https://doi.org/10.1002/aenm.201703012.

1. Introduction

The development of advanced energy storage systems (ESSs) is the promising solution for the increasing environmental concerns on fossil fuels and the inevitability of utilizing renewable energy sources.[1,2] Among them, electrochemical energy storage systems offer efficient and reliable storage of electricity, which are widely used in a range of applications from portable electronics to electric vehicles in our daily life.[3] During the past few decades, Li-ion batteries (LIBs) have occupied a dominant position of the consumer electronics market for the dramatically growing demand toward the higher energy density and long-cycle life.[4] It is estimated that the worldwide sales of LIBs will be up to 63% in all storage systems and the market value will reach $213.5 billion by 2020.[3,5] The increasing market demand for LIBs may drive the rise of cost and cause lithium resource shortage.[6] Therefore, alternative battery technologies with lower cost and more abundant resources are desirable to achieve long-term development goals.

Rechargeable Na-ion batteries (NIBs) with a similar electrochemical storage mechanism have been confirmed to be a potential alternative to LIBs for their substantial abundance of sodium reserves and low cost, which show a great competitive advantage for large-scale ESSs.[7–12] Very recently, the prototype pouch NIBs with layered $Na_{0.9}[Cu_{0.22}Fe_{0.30}Mn_{0.48}]O_2$ cathode and soft carbon anode materials (derived from anthracite), have been successfully fabricated. This Na-ion full battery exhibits an energy density of ≈100 Wh kg^{-1} with good long-cycle stability. A series of safety experiments demonstrate the pouch cells to satisfy the needs of practical applications, and most importantly, the lower cost is much desirable for the large-scale ESSs.[11] A recent review article systematically summarized the most recent developments on Na-ion full cells, which gave an academic overview of Na-ion technologies.[13] The current NIBs derived by organic liquid electrolytes (OLEs) made from sodium salts and organic solvents usually suffer from several problems, including limited electrochemical window, flammability, and leakages to the potential safety hazard in large-scale applications.[7,10,14–16]

Lithium metal as an anode material has become one of the most attractive anodes for a rechargeable battery owing to its unique specific capacity of 3860 mA h g^{-1} and lowest redox

potential of −3.04 V (Li⁺/Li) versus standard hydrogen electrode (SHE), which shows a very high electrochemical energy equivalent for LIBs.[5,17–20] Compared to lithium metal, sodium metal shows the acceptable specific capacity (1166 mA h g⁻¹) and slightly higher standard reduction potential (−2.71 V vs SHE), but it is more problematic than lithium metal owing to its high chemical reactivity with the organic electrolyte solvents.[21,22] Sodium metal anode also plays an important role for the development of high energy batteries (e.g., Na–S, Na–O₂ batteries).[23–25] However, the use of sodium metal in a practical battery may cause safety hazards, especially in the liquid electrolyte battery: dendritic sodium growth due to its uneven deposition upon charging, and further growth of dendrites may puncture the separator, leading to a short circuit eventually. Therefore, sodium metal batteries with higher energy density are limited and difficult to be improved for the current liquid electrolyte batteries. Although some strategies have been used to effectively suppress the growth of dendrites by introducing additives in current OLEs or surface protection to avoid direct contact between sodium metal and electrolytes.[21,22,26–28] The straightforward strategy is to replace liquid electrolytes with a safer electrolytic media forming physical obstacles to stop the growth of dendrites, which will indeed improve the electrochemical properties of a battery.
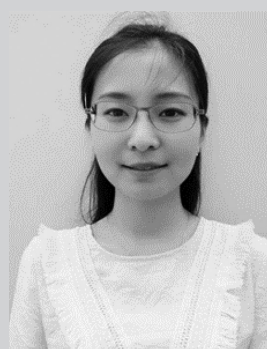
Solid-state batteries (SSBs) provide a promising choice to the next generation of devices because of their enhanced safety and accessible to high-energy and high-power densities. The conventional NIBs with liquid electrolytes and solid-state sodium batteries with solid electrolytes (in **Figure 1**a,b) generally comprise four components: cathode, anode, electrolyte, and separator materials; while in the case of solid batteries, solid-state electrolytes (SSEs) can be served as electrolyte and separator simultaneously. However, several challenges should be further understood and solved in the development of SSEs, including a high ionic conductivity (>10⁻² S cm⁻¹), chemical stability conjugating with anode and cathode materials, appropriate electrochemical stability window, mechanical property, etc.[29–35] Solid–solid interface between electrode and solid electrolyte materials is the key factor, which determines the electrochemical performance of a solid-state battery. In this review, we will provide a comprehensive summary on Na-ion SSEs in Section 2, where the ion-transport mechanisms will be discussed and the analysis on the fundamental properties including ionic conductivity, chemical/electrochemical stability, mechanical property, preparation process will be introduced based on the representative examples. In Section 3, the recent development on SSBs will be overviewed; and in Section 4, the considerations and future perspectives such as sodium metal anode, interfacial stability, safety, energy and power densities, and long-term cycling stability, will be discussed. Nevertheless, sodium-based SSBs are being the potential applications for large-scale ESSs, which would capture widespread attention.

Chenglong Zhao received his B.S and B.Admin. degrees from China University of Geosciences in Beijing, in 2015. Currently, he works as a postgraduate researcher following Prof. Yong-Sheng Hu in Institute of Physics, Chinese Academy of Sciences (IOP-CAS) on novel energy storage and conversion materials. His research interests focus on the preparation and characterization of inorganic crystal materials.

Yaxiang Lu received her Ph.D. degree at University of Birmingham (UK), and then she moved to University of Surrey (UK) to work as the research fellow. After that she was awarded the International Young Scientist Fellowship by the Institute of Physics, Chinese Academy of Sciences (IOP-CAS) following Prof. Yong-Sheng Hu. Her research interests focus on advanced materials for energy storage and conversion, such as noble metal based electrodes for polymer electrolyte fuel cells and new materials for sodium batteries.

Yan Yu is working in the University of Science and Technology of China (USTC). She received her Ph.D. in material science at USTC in 2006. From 2007 to 2008, she worked as a postdoctoral at Florida International University. After that she received Humboldt Research Fellowship and the Sofja Kovalevskaja award from the Alexander von Humboldt Foundation and worked at the Max Planck Institute for Solid State Research in Stuttgart, Germany. Her current research interests mainly include design of novel nanomaterials for clean energy, especially for batteries and the fundamental science of energy storage system.

2. Solid-State Electrolytes

Generally, SSEs can be divided into three main categories: solid polymer electrolytes (SPEs), composite polymer electrolytes (CPEs) and inorganic solid electrolytes (ISEs). SPEs made up of the polymer matrix and sodium salt form a macromolecular architecture, possessing low flammability, good flexibility, and great competitive advantage in flexible solid-state sodium batteries (in Figure 1c).[36,37] SPEs based on the polyethylene oxide (PEO) integrated with sodium salts are widely investigated in
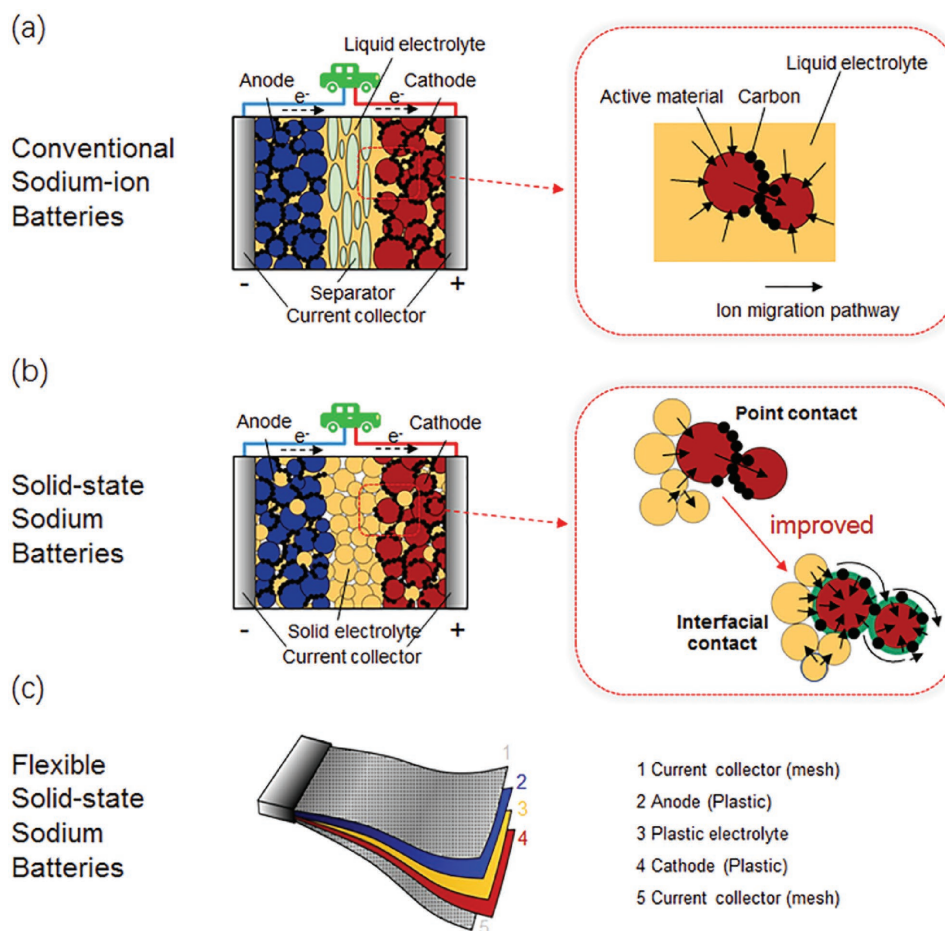
Figure 1. Illustrations of representative a) organic liquid electrolytes (OLEs), b) inorganic solid electrolytes (ISEs), and c) solid polymer/plastic electrolytes (SPEs) for conventional sodium-ion batteries (NIBs) and solid-state sodium batteries. The electrode–electrolyte interface layers are highlighted for attention. Adapted with permission.[30] Copyright 2016, Macmillan Publishers.

solid-state sodium batteries.[38–40] However, SPEs show the relatively low ionic conductivity $\approx 10^{-6}$ to 10^{-8} S cm^{-1} at room temperature (RT). In order to solve this problem, CPEs was prepared by adding ceramic fillers (e.g., SiO_2, Al_2O_3, ZrO_2) to enhance the ionic conductivity,[41–44] which can create more amorphous regions in polymer host to enhance ion transport.[45] Usually, ISEs possess intrinsic high ionic conductivity at ambient temperature ($\approx 10^{-3}$ S cm^{-1}) as well as high mechanical strength (suppressing the growth of sodium dendrites), but the high cost and complex processing need further optimization.

A high ionic conductivity of SSEs at RT is the important parameter for the development of solid-state sodium batteries. A summary of ionic conductivity for the representative sodium-ion SSEs is presented in **Figure 2**. Unfortunately, none of these materials has been discovered with the high ionic conductivity at RT, even the same level as that of liquid electrolyte (in red oval). Compared to polymer electrolytes, ISEs show a higher ionic conductivity at a relatively low temperature range. Recently, Na Super Ionic Conductor structure (NASICON) $Na_{3.3}La_{0.3}Zr_{1.7}Si_2PO_{12}$ composite electrolyte was found to have a higher ionic conductivity of 3.4×10^{-3} S cm^{-1} at 25 °C,[46] which showed a potential to develop solid electrolytes. In this section, we will provide a summary of the current Na-ion SSEs,

covering SPEs, CPEs, and ISEs, and discuss their unique ion-transport mechanisms and fundamental properties for potential SSBs.

2.1. Solid Polymer Electrolytes

Polymer electrolytes can be prepared by a dissolution of metal salts in a polymer host with relatively high molecular weight.[47–49] Alkali-ion can be solvated by polymer chains and move along with the movement of molecular chains to lead to ion transport.[50–52] However, the movement of polymer chains is seriously influenced by the temperature; e.g., polymer electrolyte could possess an ionic conductivity of 10^{-3} to 10^{-4} S cm^{-1} for a battery operation normally above 80 °C. Polymer electrolytes have good flexibility for compensating the volume changes of electrodes, making them as the promising candidates for flexible SSBs.[53] The commonly used polymer matrix for SSEs are PEO, poly(methyl methacrylate) (PMMA), poly(vinylidene fluoride) (PVDF), poly(vinylidene fluoridehexafluoropropylene), poly(vinyl chloride), poly(propylene oxide)), poly(acrylonitrile) (PAN), poly(vinyl alcohol) (PVA), in which PEO is the most widely used polymer owing to its flexible ethylene oxide
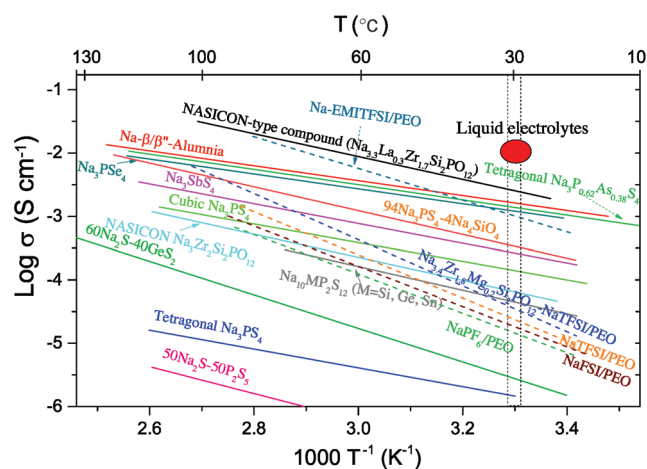
Figure 2. Summary of ionic conductivity for the representative sodium-based solid-state electrolytes (SSEs). Dashed box marks room temperature and red oval marks liquid electrolyte. Poly(ethylene oxide) (PEO), Na super ionic conductor structure (NASICON), $NaN(SO_2F)_2$ (NaFSI), $NaN(SO_2CF_3)_2$ (NaTFSI), 1-ethyl-3-methylimidazolium bis(trifluoromethanesulfonyl)imide (EMITFSI).

segments and ether oxygen atoms as well as the commercial availability.[38,39,49–56]

2.1.1. Ion-Transport Mechanisms

For these polymer hosts, polar groups (e.g., −O−, −N−, −S−, C=O, C=N) are of great importance to help dissolve sodium salts and form polymer–salt group. In fact, a higher dielectric strength for polymer matrix can often facilitate the dissociation of inorganic salts.[57] The widely accepted view is that the ion transport in SPEs mainly occurs in the amorphous regions of polymer hosts, in which the molecular chains can oscillate above their glass transition temperature (T_g), resulting in ionic conductivity.[58–60] For example, as shown in **Figure 3**a,b, Na^+ ion first locates at sites to coordinated with polar groups of polymers (e.g., −O− in PEO); under the electric field, the segmental motion of molecular chains induces free volumes for Na^+ ion migration. With the constant influence of the electric field, Na^+ ions move/hop from one coordination site to the adjacent active sites along the long chains to realize ions transport.[36,51,61] On
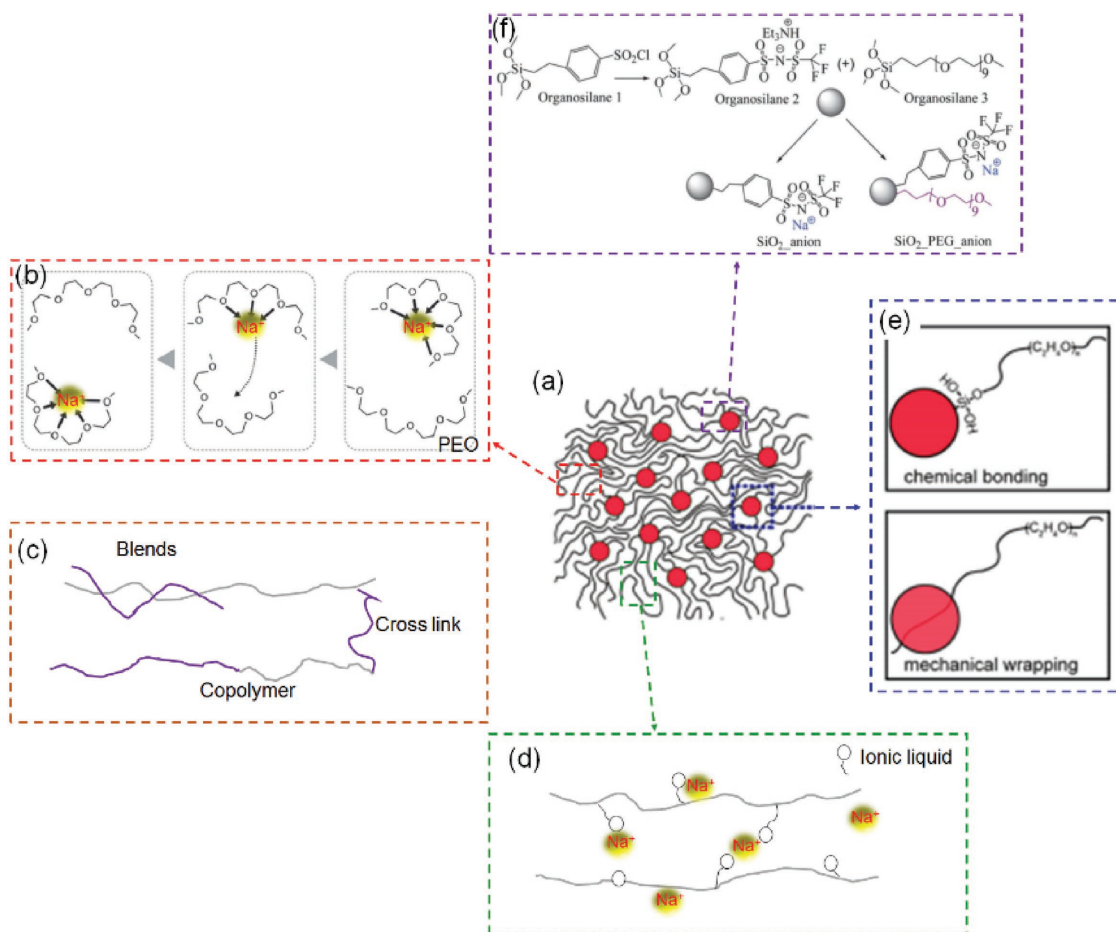

Figure 3. Schematic figures of the ion-transport procedure for polymer-based electrolytes and the common approaches for improving the performance of polymer electrolytes. a) The amorphous polymer matrix. Adapted with permission.[88] Copyright 2016, American Chemical Society. b) Ion-transport mechanisms of the selected PEO polymer. Adapted with permission.[48] Copyright 2016, The Royal Society of Chemistry. c) Models for polymer blends, copolymer, crosslink. d) Ion-transport in the ionic liquid doping polymer. e) Connection types between inorganic fillers (e.g., $Na_3Zr_2Si_2PO_{12}$, SiO_2) with polymer chains. Reproduced with permission.[88] Copyright 2016, American Chemical Society. f) The synthesis of inorganic–organic hybrid SiO_2 nanoparticles. Reproduced with permission.[91] Copyright 2013, The Royal Society of Chemistry.

the other hand, a possibility of ion transport occurring in static and ordered environment of a crystalline polymer host was reported, where Li^+ ions can move from one site to the adjacent in the cylindrical tunnels in $PEO_6:LiXF_6$ (X = P, As, Sb) crystalline polymer electrolytes without segmental motion.[62–64] However, there is no report on the crystalline polymer for ion transport in sodium-based SSEs until now. Generally, the ion transport in SSEs may not be easily understood due to lack of exact structure-property modes. In case of ion transport in polymer-based electrolytes, the mechanism is related to an ionic moving/hopping motion along with the relaxation/breathing of polymer chains,[66,67] and its temperature-dependent nature is intensively analyzed by the Arrhenius and Vogel–Tammann–Fulcher models or a combination of them.[65–67]

2.1.2. PEO-Based Electrolytes

PEO with the dissolved alkali metal salt was discovered to show ionic conductivity in 1973, which was first proposed for solid-state battery in 1979.[51,52] The first PEO-based SPEs for sodium battery was reported in 1988 with the $NaClO_4$ salt dissolved in PEO host, which showed an ionic conductivity of $\approx 3 \times 10^{-6}$ S cm^{-1} at RT.[69] After that, $NaN(SO_2F)_2$ (NaFSI)- and $NaN(SO_2CF_3)_2$ (NaTFSI)-PEO SPEs were studied for a high ionic conductivity at RT.[70,71] Currently, other sodium salts have also been studied for PEO-based SSEs, including $NaPF_6$, $NaClO_4$, $NaCF_3SO_3$, NaSCN, $NaBF_4$, sodium 2,3,4,5-tetracyano-pirolate (NaTCP), sodium 2,4,5-tricyanoimidazolate (NaTIM), etc.[40,60–73] Among these salts, NaTFSI is the relatively promising one due to its higher ionic conductivities about $\approx 10^{-4}$ S cm^{-1} above 80 °C) for PEO-based SSEs.[40] It was reported that NaTFSI-PEO SPEs presented a higher RT ionic conductivity than that of NaFSI-PEO SPEs, which could be attributed to the weaker lattice energy of the NaTFSI salt and the large TFSI$^-$ group effectively reducing the crystallinity of PEO.[71] In fact, the ionic conductivity is intensively depended on the number of free Na^+ ions; NaTFSI salt can be dissolved much easier than NaFSI salt in the PEO host with more movable ions. However, NaTFSI exhibited a relatively low corrosion potential (i.e., voltage < 4 V vs Na^+/Na) of aluminum (Al) foil.[74]

2.1.3. Non-PEO-Based Electrolytes

PEO is the most widely used polymer host because of its higher solubility for sodium salts, good structural and chemical stability, especially the high ionic conductivity in amorphous region (above the melting point). However, PEO shows a low oxidation potential, poor mechanical properties and a high degree of crystallinity at ambient temperature, resulting in the low ionic conductivity.[38–40] By substituting the active group of C=O by C=N, PAN was also studied for sodium-based SSEs. $NaCF_3SO_3$-PAN SSEs show a higher ionic conductivity of $\approx 7.13 \times 10^{-4}$ S cm^{-1} at RT and a lower activation energy ≈ 0.23 eV, which can be due to the weaker interaction between Na^+ and nitrogen atom in PAN host.[75] It is difficult to be shaped into film and the mechanical strength is poor, which hinders its practical application. Semicrystalline polymer PVA was also

studied for the solid electrolyte owing to advantages of easy preparation, high dielectric constant strength and good film-forming property.[76] NaBr-PVA electrolytes with different weight ratios were prepared by a solution-casting technique, where the electrolyte with ratio of 3:7 (NaBr:PVA) showed a higher ionic conductivity of 1.36×10^{-4} S cm^{-1} at 40 °C.[76] $NaClO_3$-, $NaClO_4$-, and NaF-PVP polymer electrolyte were also prepared but without a desired ionic conductivity.[77–79]

Because of the good mechanical elasticity, SPEs can also be used as separators to segregate electrode materials or buffer layers to suppress deformation of electrode materials. Unfortunately, SPEs often suffer from a low ionic conductivity of less than 10^{-5} S cm^{-1} at RT, which is not high enough to drive the battery operation unless the temperature rising to 60–80 °C. A summary of the ionic conductivity of SSEs for sodium battery is presented in **Table 1**. Unless material innovation to be further developed, SPEs may not be suitable for the electrochemical devices operated at RT.

2.2. Composite Polymer Electrolytes

In order to further enhance the ionic conductivity of SPEs, several strategies (in Figure 3) have been implemented, including polymer crosslinking, blending, copolymerization, doping of additives such as plasticizers, ionic liquids, inorganic fillers, and liquid electrolyte.[44,50,80–88] Compared to SPEs, CPEs often provide some better properties in electrochemical devices: a high ionic conductivity benefited from more amorphous region, good flexibility, chemical/thermal stability, etc. Polymer crosslinking, blending, copolymerization are the effective ways to increase ionic conductivity, but the incorporation of inorganic fillers has attracted a wide attention for the remarkably improved ionic conductivity, and good mechanical strength. Therefore, in this work, we focus on discussing influence of the incorporation of ceramic fillers. A good review article ref. [50] on the polymer electrolytes of LIBs, including polymer crosslinking, blending, copolymerization, etc. is recommended here for reference. Incorporated with nanosized TiO_2, $NaClO_4$-PEO

Table 1. A summary of ionic conductivity for sodium-based solid polymer electrolytes (SPEs).

SPEs	[EO]/[Na]	Conductivity [S cm^{-1}] (room temperature)	Conductivity [S cm^{-1}] (80 °C)	Ref.
$NaClO_4$-PEO	12	$\approx 1.4 \times 10^{-6}$	6.5×10^{-4}	[68]
$NaPF_6$-PEO	15	5×10^{-6}	$\approx 2 \times 10^{-4}$	[69]
NaTFSI-PEO	20	4.5×10^{-6}	1.3×10^{-3}	[40]
NaFSI-PEO	6	$\approx 1.5 \times 10^{-6}$	1.3×10^{-4}	[70]
NaFNFSI-PEO	15	$\approx 2 \times 10^{-6}$	3.36×10^{-4}	[39]
NaPCPI-PEO	20	1.1×10^{-5}	5.3×10^{-4}	[73]
NaTCP-PEO	16	6.9×10^{-5}	1.57×10^{-3}	[73]
NaTIM-PEO	16	5.7×10^{-5}	7.7×10^{-4}	[73]
$NaCF_3SO_3$-PAN	4.16	7.13×10^{-4}	$\approx 5 \times 10^{-3}$	[75]
NaBr-PVA	2.3	1.36×10^{-6}	$\approx 8 \times 10^{-6}$	[77]
$NaClO_4$-PVP	3.3	$\approx 2.5 \times 10^{-6}$	$\approx 7 \times 10^{-5}$	[78]

ADVANCED
SCIENCE NEWS
www.advancedsciencenews.com

ADVANCED
ENERGY
MATERIALS
www.advenergymat.de

CPEs fabricated by a solution casting technique exhibited a higher ionic conductivity of 2.62×10^{-4} S cm^{-1} at 60 °C than that of the TiO$_2$-free SPEs (1.35×10^{-4} S cm^{-1}).[83] Beyond simply mixing inorganic fillers with polymer matrix mechanically, in situ growth of monodispersed SiO$_2$-polymer electrolytes was proposed. This synthesis method strengthens the much stronger chemical interactions between inorganic fillers and polymer chains, thus producing more amorphous regions and leading to a higher ionic conductivity.[88] Ionic liquids are typically identified as the ideal electrolyte additives for the high ion conductivity, high thermal stability and low flammability, etc.[89–92] A hybrid NaClO$_4$-PEO-5%SiO$_2$-x% Emim FSI[1-ethyl-3-methylimidazolium bis(fluorosulfonyl) imide] (x = 50, 70) solid electrolyte was reported for solid-state sodium batteries, where a high RT ionic conductivity about 1.3×10^{-3} S cm^{-1} was achieved.[44] Additionally, two special structure of SiO$_2$ groups were synthesized as shown in Figure 3f by grafting SiO$_2$ nanoparticles with sodium 2-[(trifluoromethanesulfonylimido)-N-4-sulfonylphenyl]ethyl and polyethylene glycol (PEG), forming SiO$_2$-PEG-anion and/or Na$^+$ salt (SiO$_2$-anion), respectively, and then the two groups were dissolved in the matrix of PEO and polyethyleneglycol dimethylether to obtain epoxy resin-SiO$_2$-anion and EP-SiO$_2$-PEG-anion CPEs.[91] The obtained two CPEs presented the ionic conductivity of $\approx 10^{-5}$ S cm^{-1} at RT, but EP-SiO$_2$-PEG-anion could get a higher ionic conductivity with the same Na$^+$ concentration, which could be attributed to the high-delocalized anionic sulfonimide groups suppressing the large concentration polarization. All these indicates that the proper optimization on each segment can lead to a development of better CPEs with high ionic conductivity, good mechanical properties, etc. Therefore, CPEs have the ability to achieve increased ionic conductivity to a certain extent; more importantly, their electrochemical and mechanical properties can also be improved based on proper strategies.

In addition, gel polymer electrolytes, composed of incorporating an organic electrolyte solution into a polymer matrix, can be regarded as the intermediate state between typical liquid and dry solid polymer electrolytes, which lead to a higher ionic conductivity about 10^{-4} to 10^{-3} S cm^{-1} at RT.[85–87] Compared to the organic liquid electrolytes, an improved safety is often obtained due to the limited leakage of liquid electrolyte from the polymer hosts. A gel polymer electrolyte membrane of perfluorinated sulfonic ionomer in Na form swollen with ethylene carbonate and propylene carbonate nonaqueous solvents was studied as the electrolytes and separators for NIBs.[85,86] This electrolyte showed the good mechanical and thermal stability as well as high ionic conductivity about 2.8×10^{-4} S cm^{-1}. The study shows that the high ion exchange capacity of perfluorinated sulfonic ionomer can effectively offer enough ionic sites to reduce the crystallinity and increase the absorption capacity of solvent per unit weight of membranes. In comparison with liquid electrolyte, the as-prepared polymer electrolytes exhibited a higher reversible capacity and better cycling stability with the Na$_{0.44}$MnO$_2$ as cathode and Na metal as anode.[85] Recently, hierarchical poly(ionic liquid)-based solid electrolytes were in situ prepared for high-safety LIBs and NIBs, which showed a high ionic conductivity >10^{-3} S cm^{-1} at RT and good electrochemical stability.[84] Benefiting from the features of poly(ionic liquid)s and advantages of in situ synthesis method, it provides high

ionic conductivity for the application in SSBs. However, the low mechanical strength and poor interfacial properties remain the potential challenges to overcome. Incorporation of inorganic fillers into GPEs is good strategy to enhance their mechanical strength and improve the electrochemical properties.[91]

2.3. Inorganic Solid Electrolytes

Compared to the polymer-based electrolytes, ISEs with a high ionic conductivity and a high Na$^+$ ion transference number at RT, can effectively improve battery performance for both long-term cycling and high-power density. In addition, ISEs with a much higher mechanical strength can suppress the growth of sodium dendrites, however, the low chemical/electrochemical stability may cause an unavoidable side reaction between electrolyte and electrode materials, resulting in a large interfacial impedance.[56] The widely studied ISEs for sodium batteries are Na-β/β''-alumina, NASICON and sulfide due to their high conductivity and good mechanical properties.

2.3.1. Ion-Transport Mechanisms

In inorganic electrolyte materials, the long-range or local structure is the key feature for ion transport. Mobile species need to move or hop from the local sites to adjacent sites by passing through an energetic barrier, which has a great influence on ionic mobility and conductivity.[93] Ion diffusion mechanisms follow the models of Schottky and Frenkel point defects but take place in the connected conduction pathways. Therefore, a large number of mobile species and available adjacent positions/defects, along with a lower energetic/migration barrier, as well as the suitable conduction pathways/channels are the indispensable factors for a high ionic conductivity.[93–96] For example, the well-known fast Na$^+$ conductor Na$_3$Zr$_2$Si$_2$PO$_{12}$, an aliovalent Si^{4+} substitution to P^{5+} in NaZr$_2$(PO$_4$)$_3$ can increase the concentration of mobile Na$^+$ and improve a skeleton of linked octahedra and tetrahedra, which significantly promotes the development of fast ion conductor.[97,98]

2.3.2. Oxide Solid Electrolytes

Due to the high ionic conductivity and negligible electronic conductivity, Na-β/β''-alumina has been extensively investigated as components for electrochemical devices since the discovery in 1967.[99] The emergence of Na-β-alumina has greatly promoted the commercialization of high-temperature Na/S batteries, which is the earliest commercially available battery system with a solid electrolyte. Na-β/β''-alumina has two crystal structures originating from different layer/block stacking sequences and chemical compositions shown in **Figure 4**, namely, β-Na$_2$O·11Al$_2$O$_3$ (NaAl$_{11}$O$_{17}$) and β''-Na$_2$O·5Al$_2$O$_3$ (NaAl$_5$O$_8$).[99–102] Na-β-alumina has a hexagonal structure belonging to $P6_3/mmc$ space group, while Na-β''-alumina has a rhombohedral with a space group of R-$3m$. These two structures are both stacked up by spinel blocks consisting of [AlO$_4$] tetrahedral and [AlO$_6$] octahedral, and the adjacent spinel blocks

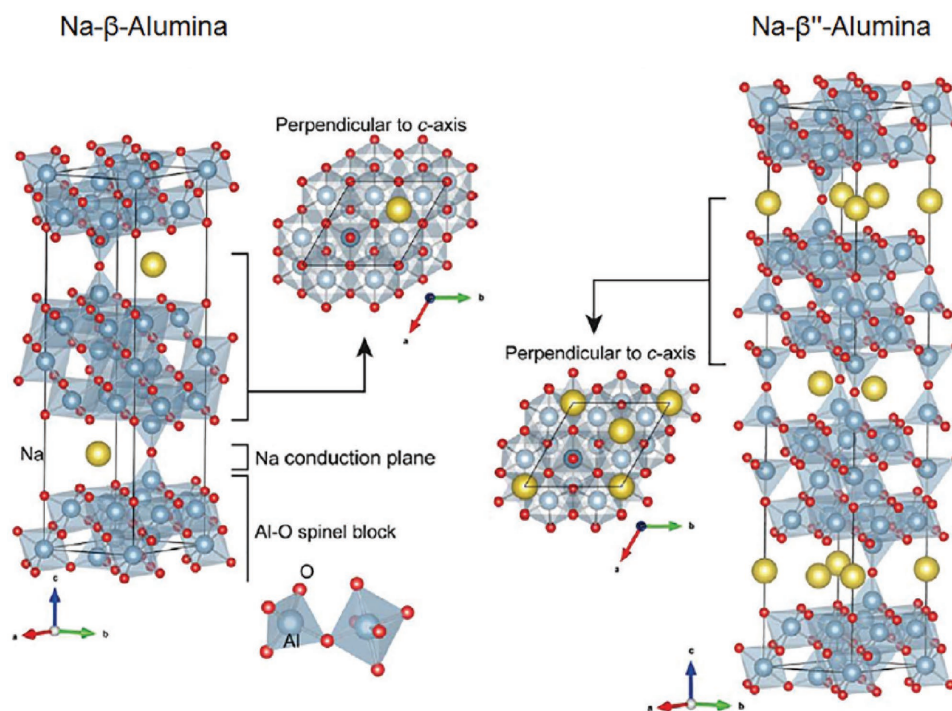**Figure 4.** Crystal structures of Na-β/β''-alumina. Reproduced with permission.[104] Copyright 2017, Elsevier.

are connected by an oxygen ion with surrounding mobile Na$^+$ to form the conduction planes. Na-β''-alumina phase with two conduction layers separated by three spinel blocks has a long c axis, which is 1.5 times longer than that of Na-β-alumina phase. In each conduction layer, Na-β''-alumina phase has two mobile Na$^+$ while Na-β-alumina phase has only one mobile Na$^+$. The bridging oxygen ion in Na-β''-alumina phase has a weaker electrostatic force with the surrounding Na$^+$, which makes it a higher ionic conductivity $\approx 2 \times 10^{-3}$ S cm^{-1} at RT.[99–102] Unfortunately, Na-β''-alumina phase is not easily prepared for its unfavorable thermodynamic stability; it usually decomposes into Al$_2$O$_3$ and Na-β-alumina mixture at high temperatures about 1500 °C (the same temperature for phase formation).[103] Thus, the obtained material is the mixture of Na-β''-alumina and Na-β-alumina, and the ionic conductivity is intensively related to the ratio of them. In order to obtain a higher proportion of Na-β''-alumina for a higher ionic conductivity, various compounds, including Li$_2$O, MgO, TiO$_2$, ZrO$_2$, Y$_2$O$_3$, MnO$_2$, SiO$_2$, Fe$_2$O$_3$, etc. are widely used as the stabilizers to suppress the formation of Na-β-alumina phase.[104–109] In addition, the accommodation of excessive sodium in the interstitial sites can also promote the formation of Na-β''-alumina toward a higher ionic conductivity. So far, different synthesis methods, such as solid-state reaction, coprecipitation, sol–gel, solution combustion techniques, alkoxide hydrolysis, molecular beam epitaxy, laser chemical vapor deposition, etc. are used to synthesize this material, and some of them can effectively decrease the grain-boundary effect leading to a higher densification.[103–114] In fact, a pure Na-β''-alumina phase is not desirable for application due to its moisture sensitivity and a low mechanical strength.[107] Na-β/β''-alumina mixture with the proper ratio and incorporated

stabilizers is more preferable for a high conductivity and good mechanical properties.

2.3.3. Sodium Superionic Conductor

NASICON as one of the most promising ionic conductors for SSBs has attracted considerable attention for its high ionic conductivity at RT.[97,98] The representative composition, Na$_3$Zr$_2$Si$_2$PO$_{12}$, is a solid solution of NaZr$_2$P$_3$O$_{12}$ with partial replacement of P by Si to form the general formula Na$_{1+x}$Zr$_2$Si$_x$P$_{3-x}$O$_{12}$ (0 ≤ x ≤ 3).[97] Na$_{1+x}$Zr$_2$Si$_x$P$_{3-x}$O$_{12}$ can form two phases of rhombohedral (R-3c) and monoclinic ($C2/c$) (1.8 ≤ x ≤ 2.2) phase shown in **Figure 5**. The monoclinic phase is the low temperature phase and can be regarded as a rotational distortion of rhombohedral phase. The two phases comprised of corner-sharing tetrahedra [SiO$_4$], [PO$_4$], and octahedra [ZrO$_6$] form a 3D network of channels for Na$^+$ transportation. Two distinct Na sites of Na1 and Na2 construct a 3D diffusion network in rhombohedral phase, while three Na sites in the distorted monoclinic phase are presented with the original Na2 splitting into Na2 and Na3 sites to form two channels of Na1–Na2 and Na1–Na3 (in Figure 5). The Na2 site in rhombohedral phase can accommodate 3 moles of Na$^+$ per formula. Therefore, a large number of mobile Na$^+$ and available adjacent vacancies can exist simultaneously, which is very beneficial for Na$^+$ diffusion. The optimal amount of Na$^+$ is related to the composition, and ≈3.3 mol Na per formula unit is a criterion to a high ionic conductivity, demonstrated by Na$_{3.3}$Zr$_{1.7}$La$_{0.3}$Si$_2$PO$_{12}$.[46,115] At this point, a distorted monoclinic phase would appear, where the less symmetry structure may be favorable for Na$^+$ migration. In addition, various
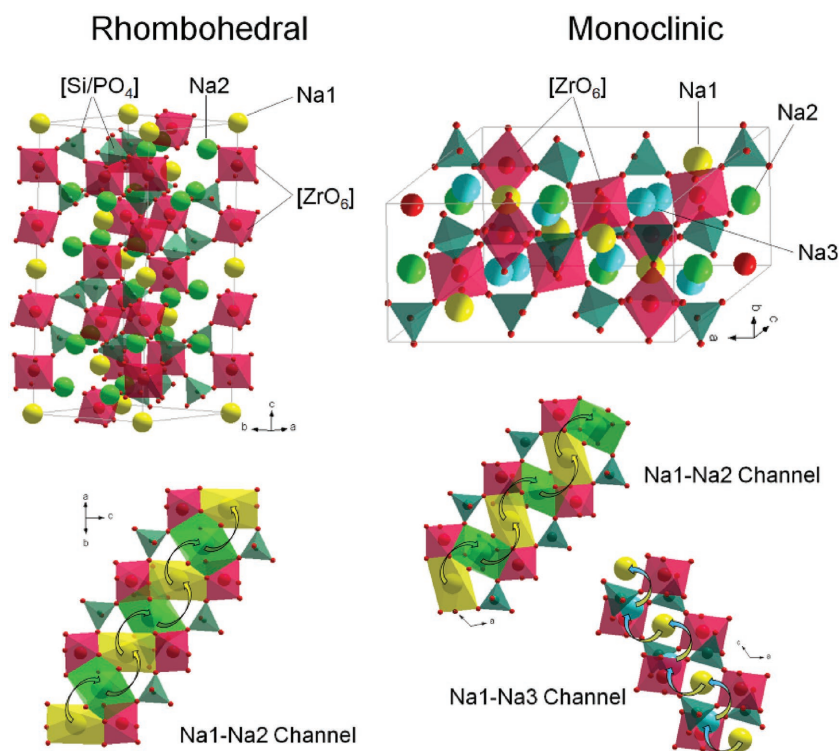
ADVANCED
SCIENCE NEWS
www.advancedsciencenews.com

ADVANCED
ENERGY
MATERIALS
www.advenergymat.de

Figure 5. Crystal structures of rhombohedral phase and monoclinic phase NASICON compounds (Na$_3$Zr$_2$Si$_2$PO$_{12}$) and their ion transport paths.

substitutions can be realized in the NASICON structure with a general formula AMP$_3$O$_{12}$, which has been reported in a comprehensive article.[115] Different compositions can lead to a great ionic conductivity gap (several orders of magnitude) in the NASICON-type compounds, where the effective ionic radius in M-sites closes to 0.72 Å.[115] Because of the closest ionic radius of Sc^{3+} (0.745 Å) and Zr^{4+} (0.720 Å), a Sc-substitution Na$_{3.4}$Sc$_{0.4}$Zr$_{1.6}$Si$_2$PO$_{12}$ was prepared by solution-assisted solid-state reaction method with a higher Na$^+$ conductivity of 4.0 × 10^{-3} S cm^{-1} at 25 °C, however, the expensive Sc is not suitable for practical applications.[116] Recently, a self-forming composited NASICON material was discovered, yielding a high ionic conductivity of 3.4 × 10^{-3} S cm^{-1} at 25 °C.[46] In Na$_3$Zr$_2$Si$_2$PO$_{12}$, a bigger La^{3+} ion was introduced to form a new phase of Na$_3$La(PO$_4$)$_2$ while it did not occupy the lattice sites of the original skeleton structure. The newly formed second phase can influence the ionic conductivity in three aspects: providing a concentration variation of the mobile ions in the pristine phase; increasing the density of the two-phase composite; facilitating the ion transport path along with the grain boundary, in this case a smaller grain boundary resistance is obtained. To be noticed, substitution of foreign elements may result in different optimal calcination temperatures, which in return would lead to a change on the density of ceramic sintering.[117–122]

2.3.4. Sulfide Solid Electrolytes

Because of the high polarizability and large ionic radius of sulfur atom weakening the interaction between skeleton

and sodium ions, sulfide solid electrolytes often provide a higher ionic conductivity at RT than that of the analogous oxides.[123] Generally, sulfide glasses are prepared by mechanical milling method followed by heat treatment, which can produce some amorphous phase surrounding the region of crystalline phase, considerably decreasing grain-boundary resistance. The composition-dependent Na$_2$S–P$_2$S$_5$ glass was prepared by mechanochemical processing, where the RT conductivity was found to be increased with the increase of Na$_2$S content (≈10^{-5} S cm^{-1} with the maximum percentage of 80%).[124] After further heat treatment, a superionic cubic Na$_3$PS$_4$ crystal (75Na$_2$S–25P$_2$S$_5$) was formed with a higher ionic conductivity of 2.0 × 10^{-4} S cm^{-1}.[124–126] Importantly, this electrolyte has a wide voltage window about ≈5 V and a good electrochemical stability against sodium metal.[125,126] Na$_3$PS$_4$ was also reported with a low-temperature tetragonal phase (P4-2$_1$c), a tetragonally distorted phase from the cubic phase (I4-3m) shown in **Figure 6**.[127] The difference of the two phases is very small, only with a less 0.2% volume change. However, in the cubic phase, only a Na1 (6b)-site occupancy is reported, while this site split into two Na$^+$ sites of Na1 (2a) and Na2 (4d) in the tetragonal structure. Both two phases were reported to have the ionic conductivity, while the cubic one shows a higher value when a glass–ceramic sample was obtained.[124–129] In addition, the introduction of vacancies can effectively improve ionic conductivity, even just 2% vacancies lead to an order of magnitude larger than that of the stoichiometric. Aliovalent doping M^{4+} (M = Si, Sn, Ge) for P^{5+} and X$^-$ for S^{2-} (X = F, Cl, Br) to induce vacancy generation were also confirmed to a feasible strategy to influence the ionic conductivity of Na$_3$PS$_4$ materials.[128,130–132] The introduction of 0.06% Si can improve the conductivity of cubic Na$_3$PS$_4$ up to 7.4 × 10^{-4} S cm^{-1}, while the Cl-doped tetragonal Na$_3$PS$_4$ (Na$_{2.9375}$PS$_{3.9375}$Cl$_{0.0625}$) shows an ionic conductivity exceeding 1.0 × 10^{-3} S cm^{-1} at RT.[130,131] Isovalent partial/complete substitution with Se^{2-} to S^{2-} or Sb^{5+}, As^{5+} to P^{5+} have also been reported, Na$_3$PSe$_4$: 1.16 × 10^{-4} S cm^{-1}, Na$_3$SbSe$_4$: 1.05 × 10^{-4} S cm^{-1}, Na$_3$P$_{0.62}$As$_{0.38}$S$_4$: 1.46 × 10^{-4} S cm^{-1}.[133–137] Although the high ionic conductivity is found for sulfide-based solid electrolytes, the stability of this kind of material, air-, or moisture-sensitivity still captures great concern. It is reported that the above sulfides are air-stable but moisture-unstable, resulting in the decrease of ionic conductivity and the release of toxic H$_2$S gas.[133,138] Recently, a high-temperature polymorph β-Na$_3$PS$_4$ was investigated combining high-temperature powder X-ray diffraction and molecular dynamics simulations, which showed that the a-Na$_3$PS$_4$ could transform to a cubic superionic phase β-Na$_3$PS$_4$ at the temperature of ≈530 K.[139] This β phase provided an expansion of bottlenecks for Na migration along c axis in the tetragonal structure making the 3D ionic transport. Two other analogues of lithium-based sulfide solid electrolytes, Na$_{10}$SnP$_2$S$_{12}$

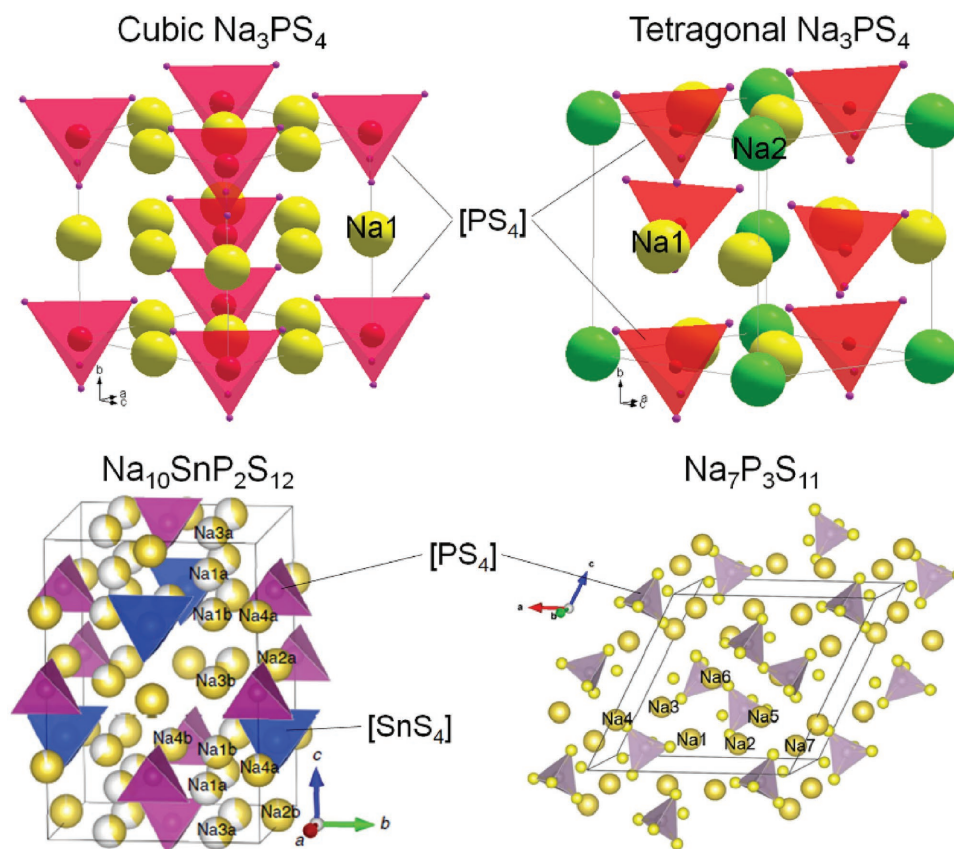**Figure 6.** Crystal structures of Na_3PS_4 (cubic and tetragonal), $Na_{10}SnP_2S_{12}$, and $Na_7P_3X_{11}$ (X = O, S, Se). $Na_{10}SnP_2S_{12}$: Reproduced with permission.[140] Copyright 2016, Nature Publishing Group. $Na_7P_3X_{11}$ (X = O, S, Se): Reproduced with permission.[141] Copyright 2017, American Chemical Society.

and $Na_7P_3X_{11}$ (X = O, S, Se), have been predicted by the powerful density functional theory calculations.[140,141] The former has been confirmed by experimental results, and the latter may not be able to synthesize due to the unfavorable thermodynamic factors in spite of a higher ionic conductivity. However, the actual composition of $Na_{10}SnP_2S_{12}$ remains to be further demonstrated due to the existence of impurity.

2.3.5. Others

Recently, complex borate-hydride compounds have been investigated as the promising SSEs for their higher ionic conductivity in **Figure 7**a.[142–147] This kind of compounds usually shows highly disordered polymorphs at high temperature, in which the fast reorientation of the anion can effectively promote cation mobility, leading to the high conductivity. However, the in-depth understanding of their ion-transport mechanisms as well as their thermal and electrochemical stabilities is still underway. As a novel solid electrolyte for sodium batteries, sodium-rich antiperovskites have recently been discovered due to their superionic conductivity and structural tolerance.[147,148] In the antiperovskite compounds, e.g., Na_3OBr, a large amount of Na ions can be accommodated. By aliovalent substitution of Sr^{2+} to Na^+, $Na_{2.9}Sr_{0.05}OBr_{0.6}I_{0.4}$ could show an ionic conductivity of 0.19 S m^{-1}, which could only be realized at operating at 200 °C.[148] In

addition, the enhancement of the conductivity together with Na^+ kinetic transport properties should be further investigated. Another kind of potential compounds with a general formula $Na_5MSi_4O_{12}$ (M = Sc, Y, Fe, In, rare earths, etc.) may be used as the solid electrolytes for sodium batteries due to their open structure for Na^+ location and migration in Figure 7b.[149,150]

In contrast to SPEs and CPEs, ISEs present a higher ionic conductivity which can drive a battery to operate at RT to some extent. However, it is not enough to contribute a good performance in terms of high power densities and long-term cycling. In Na-β/β''-alumina, by introduction of stabilizers, such as Li_2O, MgO, ZrO_2, SiO_2, etc. a higher proportion of Na-β''-alumina can be obtained with a higher ionic conductivity. For NASICON ionic conductor, due to its large 3D network and high tolerance in crystal structure, alio- and isovalent ion substitution can often increase their ionic conductivity. In addition, La^{3+} ion doping has been reported to induce the formation of a new phase to adjust the concentration of mobile ions and reduce grain boundary resistance, successfully leading to a higher ionic conductivity.[46] For sulfide, the introduction of vacancies can effectively improve ionic conductivity. Looking for new materials with higher ionic conductivity of ≈10^{-2} S cm^{-1} is the target in the near future.

In addition to the ionic conductivity, chemical and electrochemical stability are also considerably important in the discovery of electrolyte materials for sodium batteries. Commonly, several aspects need to be noted, for instance, properties
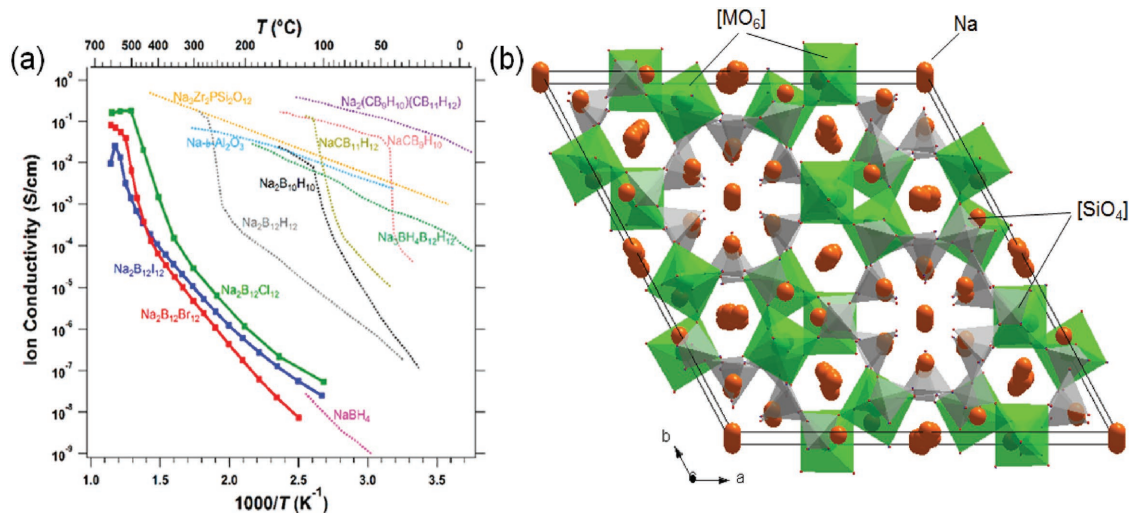
Figure 7. a) Ion conductivity of sodium–borane compounds. Reproduced with permission.[143] Copyright 2017, American Chemical Society. b) Crystal structures of $Na_5MSi_4O_{12}$ (M = Sc, Y, Fe, In, rare earths, etc.) compounds.

of electrolyte materials, electrochemical oxidation/reduction potential and interface behavior between electrolytes and electrodes. Although sulfide electrolytes show higher conductivities than the others, they often suffer from a lower chemical stability. When exposed to air or moisture atmosphere, sulfides may be decomposed, resulting in the generation of H_2S, or reaction with water to form crystalline hydrates.[124,125,133,151] By partially replacing P with alloying element arsenic (As) to obtain $Na_3P_{0.62}As_{0.38}S_4$, an increased moisture stability was attained. The improved stability could be attributed to the effectively tailoring reaction products into the difficult-forming hydrates (e.g., $Na_3P_{1-x}As_xS_4 \cdot nH_2O$) instead of the easy-forming oxysulfides (e.g., $Na_3P_{1-x}As_xOS_3$ and $Na_3P_{1-x}As_xO_2S_2$ with H_2S release) due to the weaker As–O affinity to that of P–O.[139] The moisture stability of the sulfide is based on hard/soft acids and bases theory, where P (hard acid) is preferable to react with O (hard base) instead of S (soft base).[138] Therefore, substitution P (hard acid) with antimony Sb (soft acid) have been indicated as a possible way to realize the air stability.[133] Meanwhile, the composition is also a sensitive factor.[151] Na-β''-alumina also suffers from the poor moisture sensitivity, where H^+/H_3O^+ ions can intercalate into the conduction planes or cause the ion exchange reaction with Na^+, resulting in the formation of the $Al(OH)_3$ and aluminum oxyhydroxides.[106,113,114,152–154] This often causes a sharp decrease of the mobile Na^+ to result in a poor Na^+ conductivity. In fact, Na-β/β'-alumina mixture with a proper ratio and incorporation of stabilizers are preferable for a high conductivity and chemical stability. By comparison, NASICON compounds are found to be stable in a moist environment. However, some elements, Zr^{4+}, Si^{4+}, etc. may be easily reduced at low potentials when contacted with sodium metal. SPEs and CPEs have good chemical and electrochemical stability, but suffer from a low oxidation voltage and limited thermal stability. In order to improve chemical and electrochemical stability, interface behavior is of great importance especially when contacted with sodium metal.

In addition, ISEs such as Na-β/β''-alumina and NASICON often show a high elastic modulus, which can effectively inhibit the growth of sodium dendrites to achieve improved safety. However, the high-modulus electrolytes may not usually provide a good wettability to electrode materials due to the poor interfacial contact, leading to a poor cycle performance.[28] During the battery operation, the volume change of electrode materials is inevitable, so a suitable SSE is very important for forming the favorable contacts at the time. Polymer electrolytes have a low mechanical strength thus can present a good wettability on the surface of electrode materials. Unfortunately, they are often unable to prevent the growth of metal dendrites effectively. To solve this problem, incorporation of inorganic fillers, or formation of a block copolymer to develop CPEs are the promising strategy. The preparation of composite SSEs with polymer electrolytes can be a trade-off to get the suitable modulus and surface wettability for practical application.[155–157] PEO based $Na_{3.4}Zr_{1.8}Mg_{0.2}Si_2PO_{12}$ composite electrolyte was prepared, which shows a high mechanical strength and an improved ionic conductivity.[157] In the solid-state $Na_3V_2(PO_4)_3$/CPE/Na battery, it shows the good cycle performance with negligible capacity loss over 120 cycles. In addition, the use of a small amount of ionic liquid as the interface wetting agent has been confirmed an effective mean for both SSEs and CPEs to obtain a good wettability.[158–160] Recently, a toothpaste-like electrode was developed by adding the ionic liquid into the cathode material to construct a wet interface layer with ISEs (Na-β''-alumina) to increase surface wettability toward a superior stability and high reversibility for SSBs (in **Figure 8**a).[158] Differently, formation of a wet interfacial interlayer (sodium conductive thin layer) on the surface of $Na_3Zr_2Si_2PO_{12}$ solid electrolyte by in situ heat treatment was also found to be an effective strategy to improve the poor surface wettability of SSEs in Figure 8b.[160] Furthermore, a polymer/NASICON/polymer sandwich architecture could provide a chance to increase the surface wettability of SSEs as well, which not only effectively lowered the interface resistance but also suppressed growth of sodium dendrites.[159,161] Sulfide electrolytes
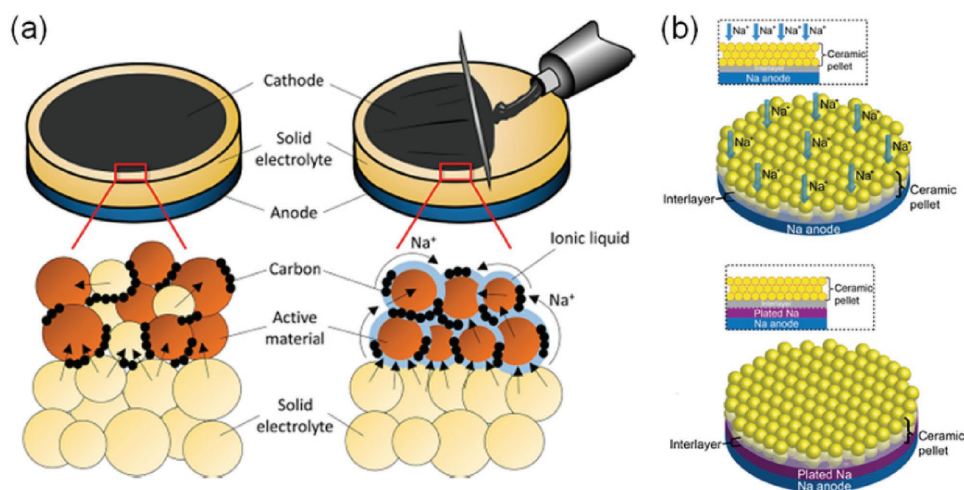
Figure 8. a) Schematic diagrams of a conventional sintering type and the designed type solid-state battery based on an inorganic ceramic electrolyte. Reproduced with permission.[158] Copyright 2017, American Chemical Society. b) Contact model of a good wetting ability artificial interlayer during the plating of sodium. Reproduced with permission.[170] Copyright 2017, American Chemical Society.

with a moderate mechanical strength are expected to serve as an interface buffer to solve the volume changes of electrode materials for a better cycle performance, even the cold-pressing treatment could lead to a better densification.[162]

3. Solid-State Sodium Batteries

The ultimate goal of developing SSEs technology is to make them successfully applied in SSBs, realizing the high safety, higher energy/power densities and long-cycle performance. In this section, we will summarize and discuss the current solid-state sodium batteries based on the above SSEs.

Na-β''-alumina is the pioneer of solid electrolytes used in sodium batteries due to its high ionic conductivity, and the high-temperature sodium–sulfur battery was discovered based on it.[98,163] Recently, the room temperature Na/S batteries based on the Na-β''-alumina solid electrolyte were also reported.[164] The batteries were constructed by sulfur/carbon (S/C) cathode, Na-β''-alumina solid electrolyte and sodium metal anode with an optimized amount of tetraethylene glycol dimethyl ether between the solid electrolyte and electrodes, where the solid electrolyte prevents the diffusion of sodium polysulfides into the anode sides.[165,166] This battery showed a high capacity of 600 mA h g^{-1} with coulombic efficiency close to 100%. In addition, Na-β''-alumina solid electrolyte was also used in the Na-ion batteries.[158,165–168] Solid-state sodium battery comprising of a P2-Na$_{2/3}$[Fe$_{1/2}$Mn$_{1/2}$]O$_2$ cathode, Na-β''-Al$_2$O$_3$ electrolyte, and Na$_2$Ti$_3$O$_7$/La$_{0.8}$Sr$_{0.2}$MnO$_3$ composite anode were prepared and showed a reversible capacity of 152 mA h g^{-1} at 350 °C.[169] Furthermore, a solid-state battery was investigated based on the layered oxide Na$_{0.66}$Ni$_{0.33}$Mn$_{0.67}$O$_2$, Na-β''-alumina and sodium metal as cathode, electrolyte, and anode, respectively, which showed an outstanding rate capability and an ultralong cycle life of 10 000 times with a capacity retention of 90% at 6 C rate at 70 °C (in **Figure 9**a). Additionally, this SSB also

presented a good performance at RT except for a poor power density.[158] The outstanding performance was attributed to the design of toothpaste-like electrode which could adhere onto the surface of solid electrolyte and keep interface well contact with SSEs.

Similar to the Na-β''-alumina, NASICON-type electrolytes also present a high ionic conductivity but suffer from a big interface resistance in the SSBs. Na/Na$_3$Zr$_2$Si$_2$PO$_{12}$/Na$_3$V$_2$(PO$_4$)$_3$ SSBs were evaluated at high temperature as shown in **Figure 10**a, which exhibited a poor rate and cycle performance.[168] Na/Na$_{3.3}$Zr$_{1.7}$La$_{0.3}$Si$_2$PO$_{12}$/Na$_3$V$_2$(PO$_4$)$_3$ batteries were also studied and operated at 80 °C in Figure 10b, where composite cathode was prepared by mixing Na$_3$V$_2$(PO$_4$)$_3$ with electrolyte powder and carbon and then cosintered with electrolyte pellet under 700 °C for 2 h before cell assembling. It displayed a reversible capacity of 107.4 mA h g^{-1} at the first cycle, but a capacity degradation and polarization increasing were found in the following cycles.[46] The above inferior electrochemical performance could attribute to poor contact between the electrode materials and solid electrolyte, especially during the long-term cycling process.[46] Although NASICON electrolytes possesses the high ionic conductivity and high elastic modulus, the poor wettability to electrode materials often result in the unacceptable performance for SSBs, even at a high temperature. Three strategies could be adopted to solve this problem, including the ionic liquid addition, polymer infiltration, and in situ heat treatment.[46] Figure 10c shows the electrochemical performance of a NaTi$_2$(PO$_4$)$_3$/H-NASICON/Na battery, demonstrating a good long cycling and rate performance with the Coulombic efficiency around 99.8% at all three C-rates after the initial formation cycles when operated at 65 °C. The authors showed the good performance resulting from the in situ formation of a sodium ion conductive thin layer on the NASICON electrode at a high temperature.[170] In addition, the same battery with the addition of a small amount of ionic liquid between cathode and SSEs was tested, which showed an excellent rate and long
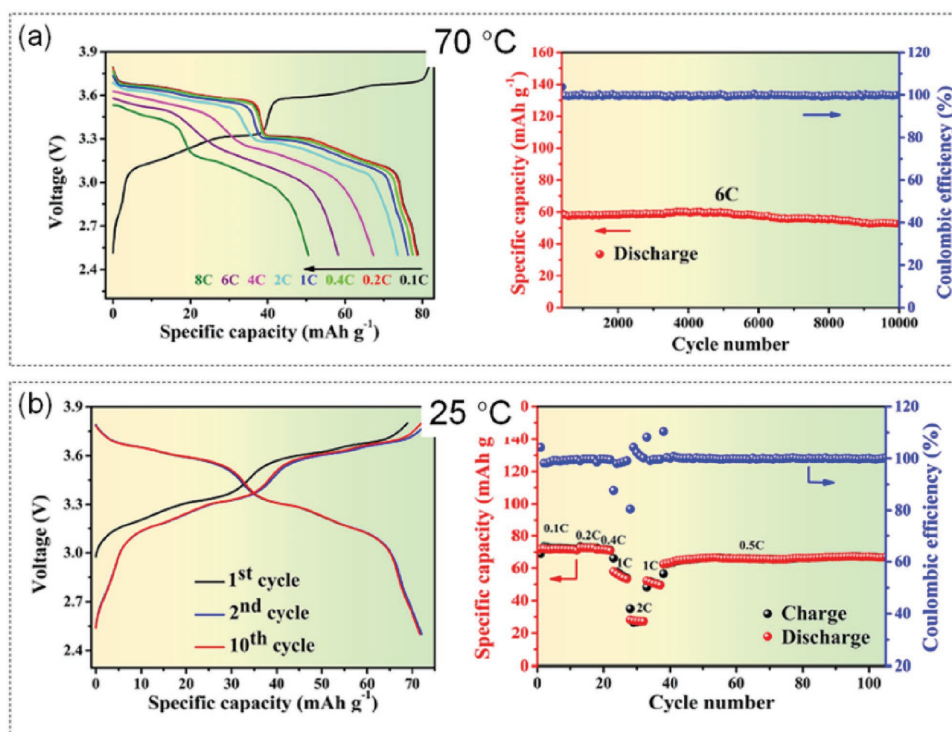
**ADVANCED
SCIENCE NEWS**

www.advancedsciencenews.com

**ADVANCED
ENERGY
MATERIALS**

www.advenergymat.de

Figure 9. Electrochemical performance of $Na_{0.66}Ni_{0.33}Mn_{0.67}O_2$/Na-$\beta''$-alumina/sodium metal SSB a) at 70 °C and b) at RT. Reproduced with permission.[158] Copyright 2017, American Chemical Society.

cycling performance, even without attenuation of the capacity after 10 000 cycles at a current rate of 10 C in Figure 10d. All of these can be ascribed to the enhanced interface contact and the formation of buffer layer between electrode materials and solid electrolytes, which can effectively reduce interface resistance and inhibit volume changes of cathode material toward an outstanding electrochemical performance.

Sulfide electrolytes with a moderate mechanical strength can be expected to have a better contact with electrode materials for a better cycle performance.[171,172] $Na_3P_{0.62}As_{0.38}S_4$ was reported with an improved moisture stability and a high ionic conductivity $\approx 1.46 \times 10^{-3}$ S cm^{-1} at RT, and a solid-state battery Na-Sn/$Na_3P_{0.62}As_{0.38}S_4$/TiS$_2$ with it as the electrolyte was fabricated.[134] Charge–discharge curves of this battery are shown in **Figure 11**a, and a large irreversible capacity with a low initial Coulombic efficiency of 72.4% and a constant degradation during the following nine cycles can be observed. Additionally, $Na_{2+2\delta}Fe_{2-\delta}(SO_4)_3$/$Na_{3.1}Sn_{0.1}P_{0.9}S_4$/$Na_2Ti_3O_7$ was prepared and showed an improved performance.[171] At a low rate, it delivered a high capacity of ≈ 113 mA h g^{-1} approaching to the theoretical value with a high Coulombic efficiency. When charged/discharged at a rate of 2 C, this battery showed a higher capacity ≈ 109 mA h g^{-1} at 80 °C than that of ≈ 83 mA h g^{-1} at RT shown in Figure 11b. After 100 cycles at the 2 C rate at 80 °C, 80% of the initial capacity was retained. Furthermore, Na_3PS_4 as both solid electrolyte and active material was proposed to form the intrinsic interfacial contact between electrolytes and electrodes.[172] The solid-state sodium–sulfur battery Na–Sn–C/Na_3PS_4/Na_3PS_4–Na_2S–C with a homogeneous Na_3PS_4–Na_2S–C nanocomposite cathode delivered a high reversible capacity of

869.2 mA h g^{-1} at 60 °C as shown in Figure 11c. A recent study showed that the sulfide electrolytes, e.g., Na_3PS_4 can be decomposed against sodium metal, resulting in an increasing overall resistance.[172]

Compared to the ISEs, polymer-based solid electrolytes usually present a good wettability on the surface of electrode materials. Therefore, development of SSBs based on polymer-based solid electrolytes has attracted an extensive attention.[39,40,44,83,84,160] However, their low mechanical strength and ionic conductivity are the potential problems for high power density and long-cycle life. Recently, NaFSI/PEO blended polymer electrolyte was prepared and showed the good interfacial stability and high electrochemical stability with sodium metal.[39] NaFSI/PEO-based NIBs with $Na_{0.67}Ni_{0.33}Mn_{0.67}O_2$ or $Na_3V_2(PO_4)_3$ as cathodes and sodium metal as anode were investigated in detail, and these two SSBs were able to normally operate at 80 °C with a high Coulombic efficiency in **Figure 12**a. However, in contrast to $Na_{0.67}Ni_{0.33}Mn_{0.67}O_2$ cathode used in Na-β''-alumina-based solid battery, the moderate cycle performance should be further improved, which could be due to the catalytic reaction between transition metal elements and PEO. The similar phenomenon also existed in other polymer-based SSBs.[39,40,44,83,84] For example, after 150 cycles at 1 C, only 70% of the capacity was retained in Na/NaFNFSI-PEO/$NaCu_{1/9}Ni_{2/9}Fe_{1/3}Mn_{1/3}O_2$.[39] Nevertheless, polymer-based electrolytes are the promising candidates for the development of the flexible SSBs. A crosslinked PMMA electrolyte with good mechanical strength was reported; the obtained Sb/Gel-PMMA/$Na_3V_2(PO_4)_3$ SSBs exhibited a
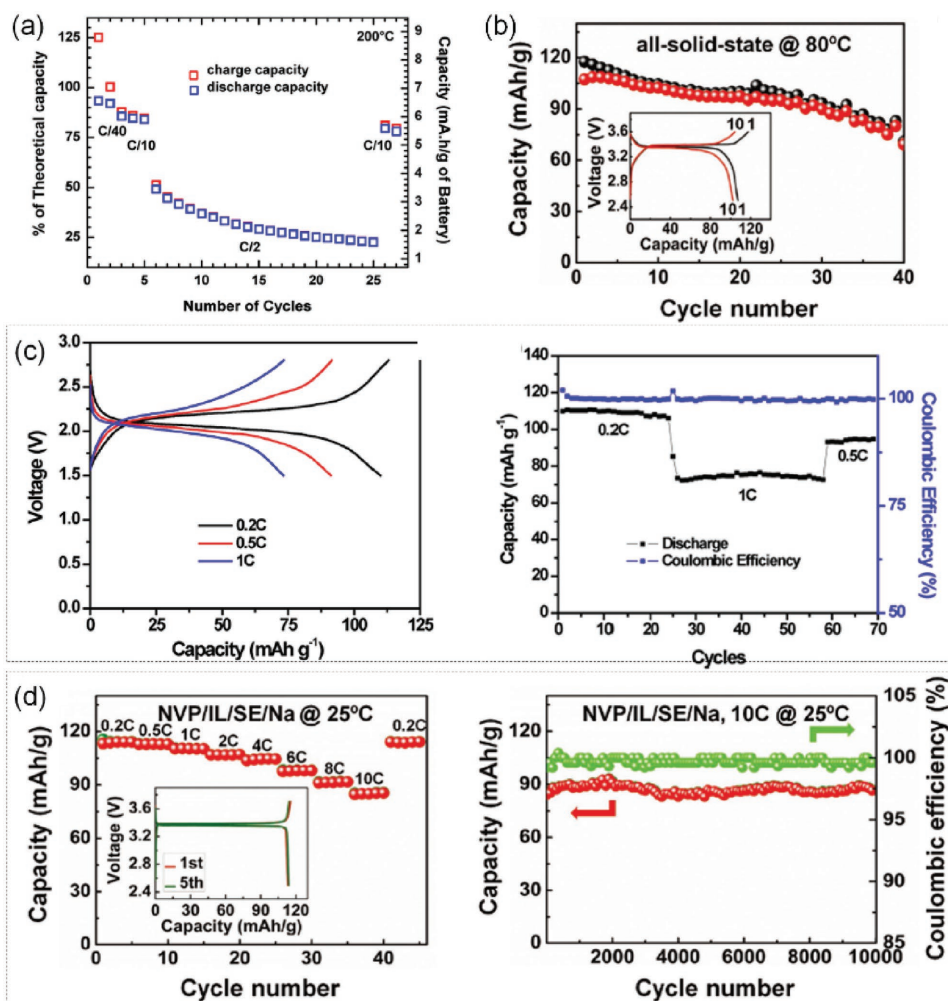
Figure 10. a) Capacity retention of $Na/Na_3Zr_2Si_2PO_{12}/Na_3V_2(PO_4)_3$ SSB over cycling at 200 °C. Reproduced with permission.[168] Copyright 2014, Elsevier. b) The cycling performance of the $Na/Na_{3.3}Zr_{1.7}La_{0.3}Si_2PO_{12}/Na_3V_2(PO_4)_3$ battery operated at 80 °C, the inset displays the charge–discharge curves of the 1st and 10th cycles at 0.1 C rate. Reproduced with permission.[46] Copyright 2016, Wiley-VCH Verlag GmbH & Co. KGaA, Weinheim. c) Charge–discharge voltage profiles and cycling performance of $NaTi_2(PO_4)_3/H$-NASICON/Na battery at different C-rates and 65 °C. Reproduced with permission.[170] Copyright 2017 American Chemical Society. d) Rate and cycling performance of the $Na/Na_{3.3}Zr_{1.7}La_{0.3}Si_2PO_{12}/ionic$ liquid/$Na_3V_2(PO_4)_3$ battery at room temperature. Reproduced with permission.[46] Copyright 2016, Wiley-VCH Verlag GmbH & Co. KGaA, Weinheim.

superior cycling stability even compared to the conventional liquid electrolyte battery shown in Figure 12 (b).[142] However, this kind of SPEs presented a poor interface contact with electrode materials, which needed the assistance of liquid electrolytes to increase the compatibility. The study on solid-state sodium batteries is just at an early stage, and related work remains to be further explored. The current reported sodium batteries based on the above SSEs are summarizes in **Figure 13**.

4. Considerations and Future Perspectives for Solid-state Sodium Batteries

SSBs are regarded as the promising alternatives to liquid batteries with the prospect for large-scale applications. Unfortunately, the relevant technologies and fundamental

studies are still in its infancy and the further development is needed. At present, several factors including interface effect, energy and power density, safety concern, etc. need to be taken into consideration, where the interface effect between electrode and solid electrolyte materials is the most critical issue, which restricts the charge-transfer process and directly influences the electrochemical performance of SSBs. In the following session, some considerations for the above-mentioned factors will be discussed, respectively, and the perspectives for the future development of SSBs are provided accordingly.

4.1. Interface

An ideal interface between electrolyte and electrodes should present good compatibility and suitable mechanical strength
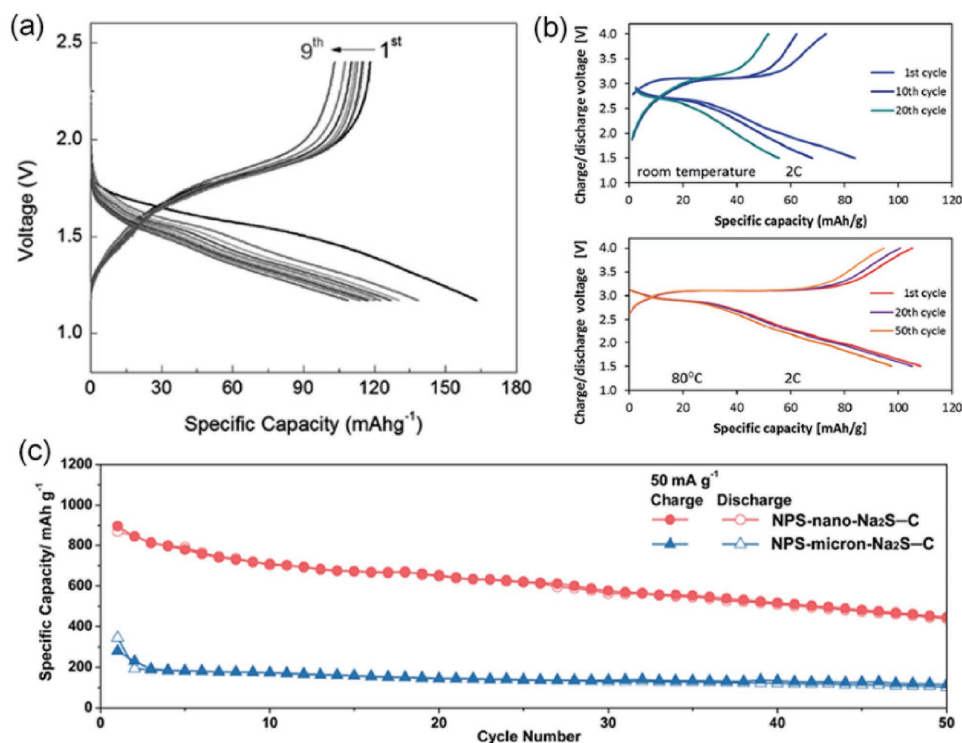
Figure 11. a) Charge–discharge curves of solid sodium battery Na-Sn/Na$_3$P$_{0.62}$As$_{0.38}$S$_4$/TiS$_2$ at the current density of 4.8 mA g^{-1} at 80 °C. Reproduced with permission.[134] Copyright 2017, Wiley-VCH Verlag GmbH & Co. KGaA, Weinheim. b) Charge–discharge profiles of Na$_{2+2\delta}$Fe$_{2-\delta}$(SO$_4$)$_3$/Na$_{3.1}$Sn$_{0.1}$P$_{0.9}$S$_4$/Na$_2$Ti$_3$O$_7$ batteries at room temperature and 80 °C at a rate of 2 C. Reproduced with permission.[171] Copyright 2017, The Royal Society of Chemistry. c) Cycling performance of NPS (Na$_3$PS$_4$)-micrometer-Na$_2$S-C (micrometer-sized) composite and NPS-nano-Na$_2$S-C (nanosized) nanocomposite cathodes at a current of 50 mA g^{-1}. Reproduced with permission.[172] Copyright 2017, American Chemical Society.
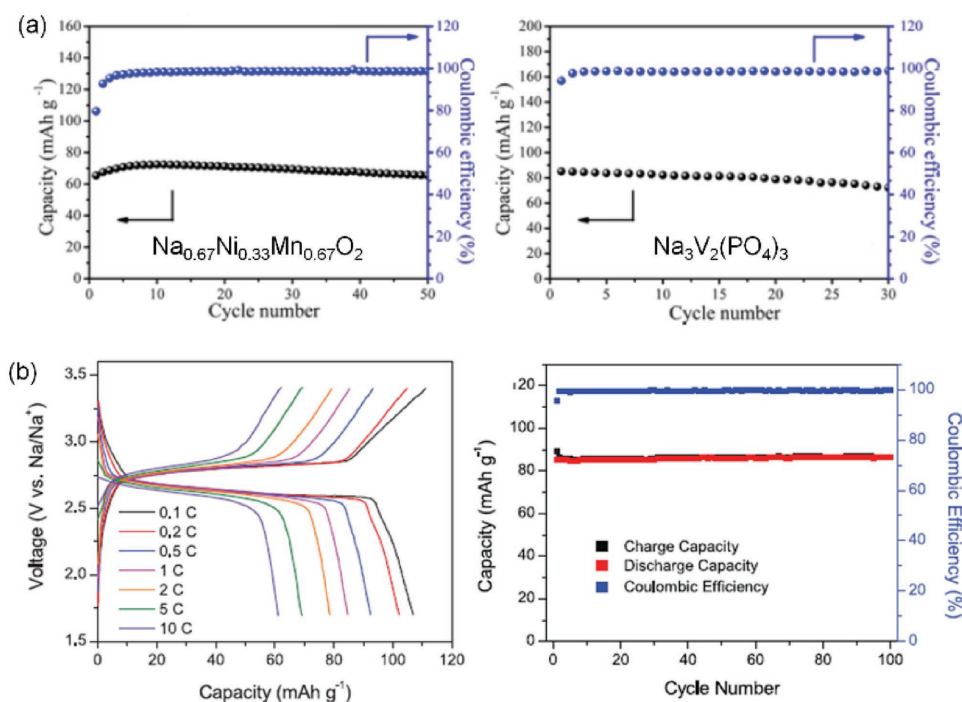
Figure 12. a) Cycling performance profiles of Na$_{0.67}$Ni$_{0.33}$Mn$_{0.67}$O$_2$ and Na$_3$V$_2$(PO$_4$)$_3$ in SPEs based SSBs tested at 80 °C. Reproduced with permission.[39] Copyright 2016, Wiley-VCH Verlag GmbH & Co. KGaA, Weinheim. b) Charge–discharge profiles at different current densities and cycling performance at a constant current density of 1 C of the sodium-ion battery Sb/Gel-SPEs/Na$_3$V$_2$(PO$_4$)$_3$. Reproduced with permission.[160] Copyright 2016, Wiley-VCH Verlag GmbH & Co. KGaA, Weinheim.

Figure 13. The relationship between specific capacity (mA h g^{-1}) and voltage (V) of the selected solid-state sodium 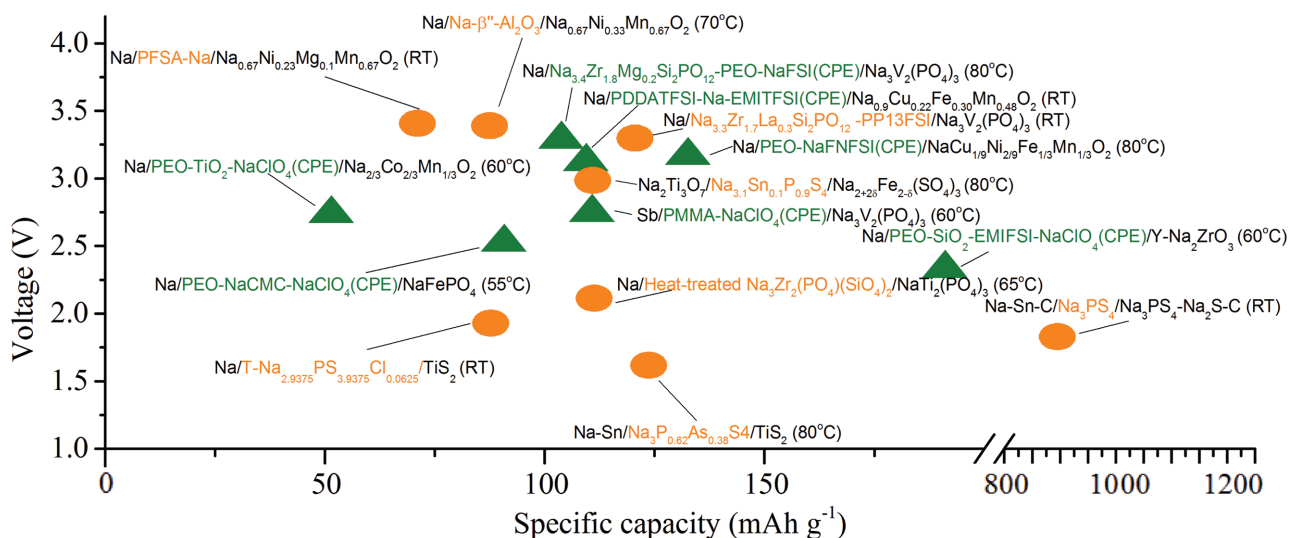batteries. Orange circle represents the SSBs based on ISEs, and the green triangle is based on polymer-based solid electrolytes.

as well as a high ionic conductivity. The good wettability can effectively form ionic conducting layer to promote the charge-transfer process. ISEs such as Na-β/β''-alumina and NASICON often show the poor compatibility with electrode material, where an effective ionic conducting layer is difficult to be in situ formed. Although the battery operated at elevated temperature has enhanced ionic conductivity, it cannot show good performance. Therefore, it is very important to form an interfacial wetting layer by the addition of ionic liquids, infiltration with polymer, and in situ/ex situ heat treatment, etc. in **Figure 14**a.[46,158,170] Diversely, sulfide electrolytes and polymer-based electrolytes have the ability to build a soft interface with electrodes, which has good ionic conductive capability and determines the good battery performance. However, their low mechanical strength or poor electrochemical stability may not be good for the long-term cycling. The large volume change of electrode material as well as the generation of side products will cause the worse compatibility, resulting in a high interfacial resistance in the long-term cycling.[39,40,44,83,84,142,160] Regarding to this feature, SSBs based on ISEs such as Na-β''-alumina and NASICON have been reported to have a good long-term stability even over 10 000 cycles. However, they suffer from poor interfacial compatibility with electrode materials, in this case, a proper interfacial wetting layer usually intends to be formed artificially by addition of little ionic liquid. Polymer-based electrolytes can provide a good interfacial compatibility, but the poor interfacial and electrochemical stability are the limitations for a long-cycle performance. A stable interface is significant to realize long-cycle performance, which not only compensates the volume changes of electrodes but also inhibits the occurrence of side reactions, even though it is still a challenge. For example, when sulfide solid electrolytes contacted with sodium metal, undesired reactions usually happens to form insulating sodium sulfide and sodium phosphide, which will lead to a higher interfacial resistance for the poor performance.[173] Thus, a highly stable sulfide against sodium metal is essential. Commonly, there are three interface layers (shown in Figure 14b) that may

be possibly formed during the initial charge–discharge process or made artificially between electrolyte and electrode materials, including a stable interface (stable), a mixed-conducting interphase (MCI), and the solid electrolyte interphase (SEI).[173] For these three interfacial layers, the stable and high ionic conductivity are highly desirable.

4.2. Energy and Power Densities

The higher energy density is a desirable feature for SSBs. A wide voltage window and good mechanical property of SSEs can provide real opportunities to develop high-voltage and large-capacity electrode materials. Metallic sodium anode with the higher capacity and low potential is the promising candidate for the high-energy SSBs. Although, most SSEs have good mechanical strength which may prevent the growth of sodium dendrites to some extent, their thermodynamical instability against sodium metal often causes some side reactions to result in serious mechanical failure. Therefore, several strategies of sodium anode modifications can be adopted, including construction of 3D framework to inhibit the volume change of sodium anode, in situ formation of artificial thin SEI layer on sodium anode surface, alloying sodium with other elements to stabilize the sodium anode, etc.[174–176] Through the above strategies, the condition of sodium metal anode was significantly improved in both carbonate and ether OLEs with less dendrite formation during the plating/stripping cycles, despite that further tests based on SSEs are needed. In addition, high-capacity/high-voltage cathode materials (e.g., polyanionic-structure compounds and anionic redox for high-capacity cathode) may be well used in SSBs to achieve higher energy density with the employment of SSEs, and in the meantime,[177,178] metal dendrites and chemical/electrochemical stability still need to be further investigated and improved. Power density is another important parameter, which indicates how fast the SSBs can be charged and discharged. The higher ionic conductivity of
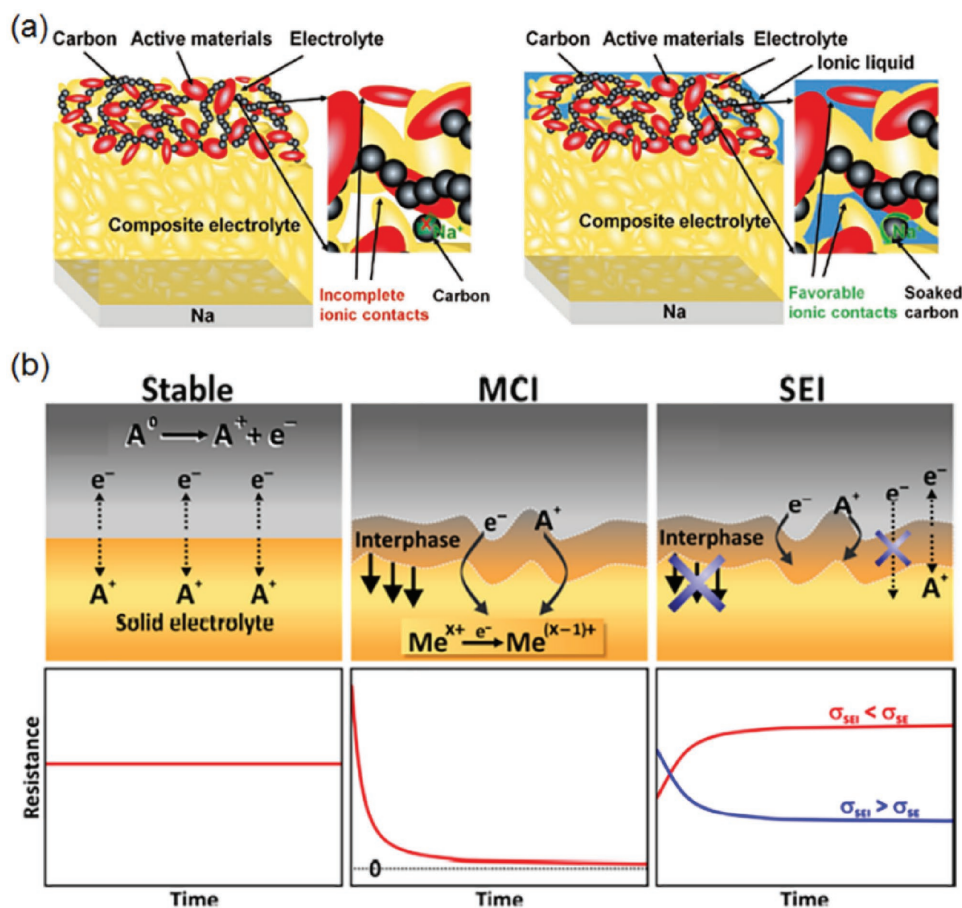
ADVANCED
SCIENCE NEWS

www.advancedsciencenews.com

ADVANCED
ENERGY
MATERIALS

www.advenergymat.de

Figure 14. a) Schematic representation of the cathode/SSEs/Na anode and cathode/IWL/SSEs/Na anode SSBs. Interfacial wetting layer (IWL) can be formed by the addition of ionic liquids, infiltration with polymer, in situ heat treatment, etc. Reproduced with permission.[46] Copyright 2016, Wiley-VCH Verlag GmbH & Co. KGaA, Weinheim. b) Illustrations of three possible interphases between electrolyte and electrode materials: a stable interface (stable), a mixed-conducting interphase (MCI), and the solid electrolyte interphase (SEI). And the corresponding time-dependent resistance is shown below. Reproduced with permission.[173] Copyright 2016, American Chemical Society.

SSEs together with good interfacial contact among all components is essential to obtain large power density. Unfortunately, the reported sodium-based SSBs all show poor power densities, which needs further effort to improve.

4.3. Safety

A major purpose on the development of SSEs is to obtain the high-safety SSBs because of the use of nonflammable solid electrolytes. In fact, sulfide electrolytes usually suffer from chemical instability in spite of a high ionic conductivity at RT. The release of toxic gas (H_2S) and the decomposition of materials imply a potential safety hazard. The same problem may happen to polymer-based materials due to their low mechanical strength and narrow limited electrochemical window, especially against sodium metal anode. Fortunately, the hazard may not happen when Na-β''-alumina and NASICON electrolytes with the high mechanical strength are employed. However, the in-depth understanding is still underway. Besides electrolyte themselves, another safety concern comes from the use of sodium metal as anode in solid-state sodium batteries.

Sodium metal, with an extremely high chemical activity, is generally considered as impractical in large-scale energy storage. However, when sodium metal is stored in an inert atmosphere or sodium anode is enclosed in a sealed solid state battery, the safety issue could be guaranteed. The safety considerations in the high chemical activity of sodium metal come from two aspects. On one hand, potential danger exists when dealing with a large amount of sodium metal in large-scale production and manufacturing due to its air and moisture sensitivity. And the improper storage or post-processed treatment may cause an unavoidable fire even explosion like lithium metal in practical use. On the other hand, once the sealed batteries were damaged, sodium metal anode would be contacted/exposed to moist air directly, giving rise to severe consequences. Here we performed a simple experiment to observe visually the evolution process of sodium metal under the environment of dry air, humid air, and water. When sodium slice is exposed to the dry air, it can be seen that a layer of sodium oxides (white color) is formed instantaneously without any change in the following time (**Figure 15**a,b), indicating sodium metal is not dangerous when used in dry air. When exposed to the humid air, the surface gradually becomes more wrinkled, and some bubbles
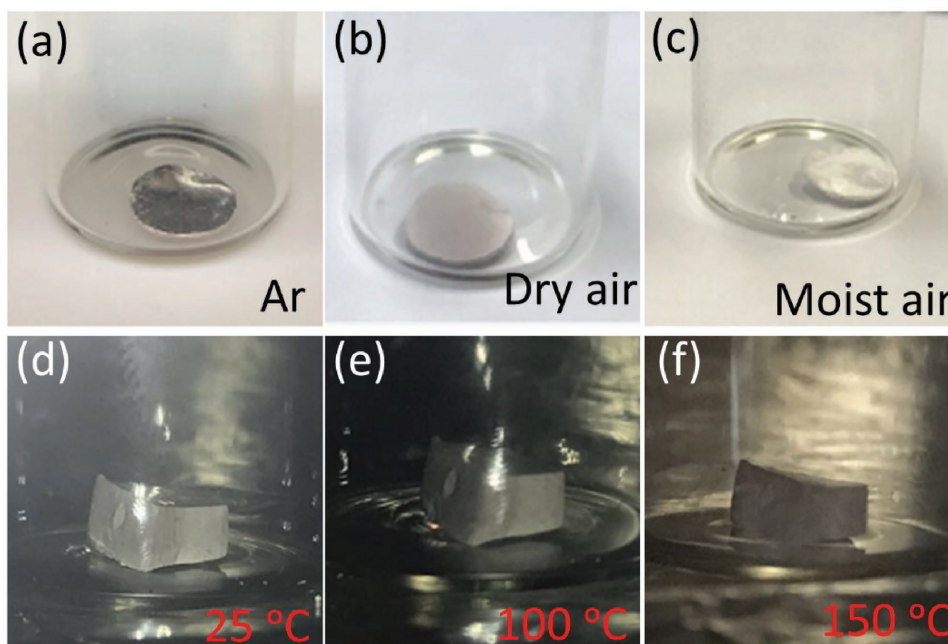
**ADVANCED
SCIENCE NEWS**
www.advancedsciencenews.com

**ADVANCED
ENERGY
MATERIALS**
www.advenergymat.de

Figure 15. Sodium metal slice in a) Ar atmosphere, b) in dry air after 20 min, and c) in moist air after 2 min. Sodium metal bulk at d) 25 °C, e) 100 °C after 10 h, and f) 150 °C after 10 h.

are generated after several minutes as shown in Figure 15c. Even like this, no drastic reaction or spark were observed during the above experimental process. However, sodium metal immediately catches fire when a drop of water is dropped on its surface. Worse still, the bottle even gets cracked due to the local temperature spiked suddenly. Therefore, it is extremely important to protect the battery system to avoid the contact of sodium anode with moisture. Another concern stems from the low melting point (97 °C) of sodium metal, which may cause internal short circuit under high working temperatures above 97 °C. In this case, another experiment was conducted by putting a sodium bulk into the vacuum oven with the temperature gradually increased. The results show that sodium metal has almost no change after 10 h at 100 °C (Figure 15e) compared to that at 25 °C (Figure 15d). When the temperature increases to 150 °C, the shape is still kept the same after 10 h (Figure 15f). No obvious melting phenomenon was observed on the surface, which is probably due to the oxide layer formed on the surface during the process of vacuuming. It remains unclear about the change under longer time (>10 h) at the constant high temperature, further investigations are still needed to clarify the issue. Looking at the phenomenon from another viewpoint, the soft characteristics of sodium metal is in turn an advantage when used in SSBs. First, it can contribute to the interfacial contact between the anode and electrolyte because the sodium anode may become soft under a higher temperature to improve the surface wettability. Second, due to the soft nature of sodium metal under the high temperature, the mechanical strength of formed dendrites may be too weak to pierce the electrolyte, indirectly improving the safety of a battery. Last but not the least, sodium metal anode may have a self-healing ability to avoid pulverization during cycling with a proper heat treatment. Therefore, whether sodium metal could be directly used

in SSBs, and how to inhibit the disadvantages and promote the advantages still remain uncertainty and worth to be investigated further. Even though the final solution has not come out yet, potential strategies like using 3D architecture to alleviate the volume change and forming protected layer to enhance the interface stability could offer promising opportunities to use sodium metal as anode to some extent. In the meantime, solid-state Na-ion batteries shall also be considered for the future development.

In this review, we systematically summarize the current sodium-based SSEs, and discuss their potential advantages and disadvantages for developing SSBs. SSEs as the promising alternative to OLEs can offer the high energy and power densities, long-term cycling and improved safety for sodium batteries. However, several challenges should be further overcome, including high RT ionic conductivity, good chemical/electrochemical stability, flexible mechanical property as well as low-cost and environmental friendly preparation process, etc. ISEs such as Na-β/β''-alumina and NASICON, present a higher ionic conductivity at RT but cannot contribute a good performance in terms of high power densities and long-term cycling due to the poor interface contact with electrode materials. A wet interfacial interlayer formed by the addition of ionic liquids, infiltration with polymer, in situ/ex situ SEI formation, etc., are effective strategies to solve this problem. In comparison, the flexible polymer-based electrolytes can easily build an ionic conduction layer with electrode materials, but their low mechanical strength and poor electrochemical stability may not be good for the long-term cycling. And the low RT ionic conductivity is not favorable to the large-scale applications. Sulfide electrolytes with a moderate mechanical strength and high RT ionic conductivity can be expected to achieve a good wettability to electrode materials for a better

**ADVANCED
SCIENCE NEWS**
www.advancedsciencenews.com

**ADVANCED
ENERGY
MATERIALS**
www.advenergymat.de

cycle performance. Unfortunately, their poor chemical stability may lead to safety hazard. Materials innovation needs to be further developed for the practical applications such as high RT ionic conductivity and high chemical and electrochemical stability. Meanwhile, interface is of great concern, which is the bridge between electrode materials and electrolytes, directly determining the batteries' performance. A good interface can effectively inhibit the growth of sodium-metal dendrites and reduce the volume deformation of sodium-metal anode, which has a profound influence on the long-term cycling. At present, the long-cycle performance seems to be available based on the reported ISEs, such as Na-β/β''-alumina and NASICON, further effort is still needed to improve the interface contact of other SSEs. In addition, high energy and power densities are also very important for SSBs toward a large-scale application. Besides discovering new materials (high-capacity and/or high-voltage cathode materials and high ionic conductivity electrolytes), sodium-metal anode might be a good choice and special design is needed when taking the safety issue into consideration. Because the study of solid-state sodium batteries is just in its infancy, related research still need to be further performed to promote the practical applications.

Conflict of Interest

The authors declare no conflict of interest.

[1] B. Dunn, H. Kamath, J. M. Tarascon, *Science* **2011**, *334*, 928.
[2] S. Chu, A. Majumdar, *Nature* **2012**, *488*, 294.
[3] J. M. Tarascon, M. Armand, *Nature* **2001**, *414*, 359.
[4] S. Chu, Y. Cui, N. Liu, *Nat. Mater.* **2017**, *16*, 16.
[5] X.-B. Cheng, R. Zhang, C.-Z. Zhao, Q. Zhang, *Chem. Rev.* **2017**, *117*, 10403.
[6] signumBox, Lithium Industry: Outlook, Perspectives, http://globalxfunds.com/ (accessed: August 2017).
[7] H. Pan, Y.-S. Hu, L. Chen, *Energy Environ. Sci.* **2013**, *6*, 2338.
[8] S. W. Kim, D. H. Seo, X. H. Ma, G. Ceder, K. Kang, *Adv. Energy Mater.* **2012**, *2*, 710.
[9] V. Palomares, P. Serras, I. Villaluenga, K. B. Hueso, J. Carretero-Gonzalez, T. Rojo, *Energy Environ. Sci.* **2012**, *5*, 5884.

[10] N. Yabuuchi, K. Kubota, M. Dahbi, S. Komaba, *Chem. Rev.* **2014**, *114*, 11636.
[11] Y. Li, Y.-S. Hu, X. Qi, X. Rong, H. Li, X. Huang, L. Chen, *Energy Storage Mater.* **2016**, *5*, 191.
[12] Y. Zheng, Y. Wang, Y. Lu, Y.-S. Hu, J. Li, *Nano Energy* **2017**, *39*, 489.
[13] W. Ren, Z. Zhu, Q. An, L. Mai, *Small* **2017**, *13*, 1604181.
[14] K. Xu, *Chem. Rev.* **2004**, *104*, 4303.
[15] K. Xu, *Chem. Rev.* **2014**, *114*, 11503.
[16] H. Che, S. Chen, Y. Xie, H. Wang, K. Amine, X.-Z. Liao, Z.-F. Ma, *Energy Environ. Sci.* **2017**, *10*, 1075.
[17] K. Zhang, G.-H. Lee, M. Park, W. Li, Y.-M. Kang, *Adv. Energy Mater.* **2016**, *6*, 1600811.
[18] P. G. Bruce, S. A. Freunberger, L. J. Hardwick, J.-M. Tarascon, *Nat. Mater.* **2012**, *11*, 19.
[19] K. Zhang, X. Han, Z. Hu, X. Zhang, Z. Tao, J. Chen, *Chem. Soc. Rev.* **2015**, *44*, 699.
[20] J.-J. Xu, Z.-L. Wang, D. Xu, F.-Z. Meng, X.-B. Zhang, *Energy Environ. Sci.* **2014**, *7*, 2213.
[21] Z. W. Seh, J. Sun, Y. Sun, Y. Cui, *ACS Cent. Sci.* **2015**, *1*, 44.
[22] A. P. Cohn, N. Muralidharan, R. Carter, K. Share, C. L. Pint, *Nano Lett.* **2017**, *17*, 1296.
[23] P. Hartmann, C. L. Bender, M. Vracar, A. K. Durr, A. Garsuch, J. Janek, P. Adelhelm, *Nat. Mater.* **2012**, *12*, 228.
[24] S. Wei, S. Xu, A. Agrawral, S. Choudhury, Y. Lu, Z. Tu, L. Ma, L. A. Archer, *Nat. Commun.* **2016**, *7*, 11722.
[25] Z. E. M. Reeve, C. J. Franko, K. J. Harris, H. Yadegari, X. Sun, G. R. Goward, *J. Am. Chem. Soc.* **2017**, *139*, 595.
[26] W. Luo, Y. Zhang, S. Xu, J. Dai, E. Hitz, Y. Li, C. Yang, C. Chen, B. Liu, L. Hu, *Nano Lett.* **2017**, *17*, 3792.
[27] Y. Zhao, L. V. Goncharova, A. Lushington, Q. Sun, H. Yadegari, B. Wang, W. Xiao, R. Li, X. Sun, *Adv. Mater.* **2017**, *29*, 1606663.
[28] D. Lin, Y. Liu, Y. Cui, *Nat. Nanotechnol.* **2017**, *12*, 194.
[29] Y. Kato, S. Hori, T. Saito, K. Suzuki, M. Hirayama, A. Mitsui, M. Yonemura, H. Iba, R. Kanno, *Nat. Energy* **2016**, *1*, 16030.
[30] Y.-S. Hu, *Nat. Energy* **2016**, *1*, 16042.
[31] P. Knauth, *Solid State Ionics* **2009**, *180*, 911.
[32] K. Fu, Y. Gong, G. T. Hitz, D. W. McOwen, Y. Li, S. Xu, Y. Wen, L. Zhang, C. Wang, G. Pastel, J. Dai, B. Liu, H. Xie, Y. Yao, E. D. Wachsman, L. Hu, *Energy Environ. Sci.* **2017**, *10*, 1568.
[33] P. Knauth, *Solid State Ionics* **2009**, *180*, 911.
[34] M. Kotobuki, H. Munakata, K. Kanamura, Y. Sato, T. Yoshida, *J. Electrochem. Soc.* **2010**, *157*, A1076.
[35] Y. Zhu, X. He, Y. Mo, *ACS Appl. Mater. Interfaces* **2015**, *7*, 23685.
[36] R. Chen, W. Qu, X. Guo, L. Li, F. Wu, *Mater. Horiz.* **2016**, *3*, 487.
[37] M. Alamgir, K. M. Abraham, *J. Electrochem. Soc.* **1993**, *140*, L96.
[38] Q. Ma, J. Liu, X. Qi, X. Rong, Y. Shao, W. Feng, J. Nie, Y.-S. Hu, H. Li, X. Huang, L. Chen, Z. Zhou, *J. Mater. Chem. A* **2017**, *5*, 7738.
[39] X. Qi, Q. Ma, L. L. Liu, Y.-S. Hu, H. Li, Z. B. Zhou, X. Huang, L. Q. Chen, *ChemElectroChem* **2016**, *3*, 1741.
[40] J. S. Moreno, M. Armand, M. B. Berman, S. G. Greenbaum, B. Scrosati, S. Panero, *J. Power Sources* **2014**, *248*, 695.
[41] F. Croce, G. B. Appetecchi, L. Persi, B. Scrosati, *Nature* **1998**, *394*, 456.
[42] C. Tang, K. Hackenberg, Q. Fu, P. M. Ajayan, H. Ardebili, *Nano Lett.* **2012**, *12*, 1152.
[43] Z. Zhu, M. Hong, D. Guo, J. Shi, Z. Tao, J. Chen, *J. Am. Chem. Soc.* **2014**, *136*, 16461.
[44] S. Song, M. Kotobuki, F. Zheng, C. Xu, S. V. Savilov, N. Hu, L. Lu, Y. Wang, W. Dong, *J. Mater. Chem. A* **2017**, *5*, 6424.
[45] M. Armand, *Solid State Ionics* **1983**, *9–10*, 745.
[46] Z. Zhang, Q. Zhang, J. Shi, Y. S. Chu, X. Yu, K. Xu, M. Ge, H. Yan, W. Li, L. Gu, Y.-S. Hu, H. Li, X.-Q. Yang, L. Chen, X. Huang, *Adv. Energy Mater.* **2017**, *7*, 1601196.
[47] S. Ramesh, S. C. Lu, *J. Appl. Polym. Sci.* **2012**, *126*, 484.

**ADVANCED
SCIENCE NEWS**

www.advancedsciencenews.com

**ADVANCED
ENERGY
MATERIALS**

www.advenergymat.de

[48] A. Varzi, R. Raccichini, S. Passerini, B. Scrosati, *J. Mater. Chem. A* **2016**, *4*, 17251.

[49] J. H. Kim, M.-S. Kang, Y. J. Kim, J. Won, N.-G. Park, Y. S. Kang, *Chem. Commun.* **2004**, *0*, 1662.

[50] K. S. Ngai, S. Ramesh, K. Ramesh, J. C. Juan, *Ionics* **2016**, *22*, 1259.

[51] D. E. Fenton, J. M. Parker, P. V. Wright, *Polymer* **1973**, *14*, 589.

[52] M. Armand, J.-M. Chabagno, M. J. Duclot, in *Fast Ion Transport in Solids: Electrodes and Electrolytes*, Vol. 5, (Eds.: P. Vashishta, J. N. Mundy, G. K. Shenoy), Elsevier, Lake Geneva, WI, USA **1979**.

[53] P. Lightfoot, M. A. Metha, P. G. Bruce, *Science* **1993**, *262*, 883.

[54] R. C. Agrawal, G. P. Pandey, *J. Phys. D: Appl. Phys.* **2008**, *41*, 223001.

[55] Y. Q. Yang, Z. Chang, M. X. Li, X. W. Wang, Y. P. Wu, *Solid State Ionics* **2015**, *269*, 1.

[56] R. Khurana, J. L. Schaefer, L. A. Archer, G. W. Coates, *J. Am. Chem. Soc.* **2014**, *136*, 7395.

[57] B. Scrosati, *Chem. Rec.* **2001**, *1*, 173.

[58] W.-S. Young, W.-F. Kuan, T. H. Epps, *J. Polym. Sci., Part B: Polym. Phys.* **2014**, *52*, 1.

[59] O. Borodin, G. D. Smith, *Macromolecules* **2006**, *39*, 1620.

[60] C. Berthier, W. Gorecki, M. Minier, M. B. Armand, J. M. Chabagno, P. Rigaud, *Solid State Ionics* **1983**, *11*, 91.

[61] M. C. Wintersgill, J. J. Fontanella, Y. S. Pak, S. G. Greenbaum, A. Almudaris, A. V. Chadwick, *Polymers* **1989**, *30*, 1123.

[62] L. Long, S. Wang, M. Xiao, Y. Meng, *J. Mater. Chem. A* **2016**, *4*, 10038.

[63] Z. Gadjourova, Y. G. Andreev, D. P. Tunstall, P. G. Bruce, *Nature* **2001**, *412*, 520.

[64] Z. Gadjourova, D. Martin, Y. Marero, K. H. Andersen, Y. G. Andreev, P. G. Bruce, *Chem. Mater.* **2001**, *13*, 1282.

[65] Z. Stoeva, I. Martin-Litas, E. Staunton, Y. G. Andreev, P. G. Bruce, *J. Am. Chem. Soc.* **2003**, *125*, 4619.

[66] R. C. Agrawal, G. P. Pandey, *J. Phys. D: Appl. Phys.* **2008**, *41*, 223001.

[67] E. Quartarone, P. Mustarelli, *Chem. Soc. Rev.* **2011**, *40*, 2525.

[68] M. A. Ratner, P. Johansson, D. F. Shriver, *MRS Bull.* **2000**, *25*, 31.

[69] K. West, B. Zachau-Christiansen, T. Jacobsen, E. Hiort-Lorenzen, S. Skaarup, *Br. Polym. J.* **1988**, *20*, 243.

[70] S. A. Hashmi, S. Chandra, *Mater. Sci. Eng., B* **1995**, *34*, 18.

[71] A. Boschin, P. Johansson, *Electrochim. Acta* **2015**, *175*, 124.

[72] R. Dupon, B. L. Papke, M. A. Ratner, D. H. Whitmore, D. F. Shriver, *J. Am. Chem. Soc.* **1982**, *104*, 6247.

[73] A. Bitner-Michalska, G. M. Nolis, G. Żukowska, A. Zalewska, M. Poterała, T. Trzeciak, M. Dranka, M. Kalita, P. Jankowski, L. Niedzicki, J. Zachara, M. Marcinek, W. Wieczorek, *Sci. Rep.* **2017**, *7*, 40036.

[74] M. M. Doeff, A. Ferry, Y. Ma, L. Ding, L. C. De Jonghe, *J. Electrochem. Soc.* **1997**, *144*, L20.

[75] Z. Osman, K. B. Md Isa, A. Ahmad, L. Othman, *Ionics* **2010**, *16*, 431.

[76] M. Mokhtar, E. H. Majlan, M. Z. M. Talib, A. Ahmad, S. M. Tasirin, W. R. W. Daud, *Int. J. Appl. Eng. Res.* **2016**, *11*, 10009.

[77] P. B. Bhargav, V. M. Mohan, A. K. Sharma, V. V. R. N. Rao, *J. Appl. Polym. Sci.* **2008**, *108*, 510.

[78] C. V. Subba Reddy, A. P. Jin, Q. Y. Zhu, L. Q. Mai, W. Chen, *Eur. Phys. J. E: Soft Matter Biol. Phys.* **2006**, *19*, 471.

[79] K. N. Kumar, T. Sreekanth, M. J. Reddy, U. V. S. Rao, *J. Power Sources* **2001**, *101*, 130.

[80] K. K. Kumar, M. Ravi, Y. Pavani, S. Bhavani, A. K. Sharma, V. V. R. N. Rao, *Physica B* **2011**, *406*, 1706.

[81] Q. Pan, Z. Li, W. Zhang, D. Zeng, Y. Sun, H. Cheng, *Solid State Ionics* **2017**, *300*, 60.

[82] C. W. Liew, R. Durairaj, S. Ramesh, *PLoS One* **2014**, *9*, 0102815.

[83] Y. L. Ni'mah, M.-Y. Cheng, J. H. Cheng, J. Rick, B.-J. Hwang, *J. Power Sources* **2015**, *28*, 37.

[84] D. Zhou, R. Liu, J. Zhang, X. Qi, Y.-B. He, B. Li, Q.-H. Yang, Y.-S. Hu, F. Kang, *Nano Energy* **2017**, *33*, 45.

[85] C. Cao, W. Liu, L. Tan, X. Liao, L. Li, *Chem. Commun.* **2013**, *49*, 11740.

[86] C. Cao, H. Wang, W. Liu, X. Liao, L. Li, *J. Hydrogen Energy* **2014**, *39*, 16110.

[87] H. Hou, Q. Xu, Y. Pang, L. Li, J. Wang, C. Zhang, C. Sun, *Adv. Sci.* **2017**, *4*, 1700072.

[88] D. Lin, W. Liu, Y. Liu, H. R. Lee, P.-C. Hsu, K. Liu, Y. Cui, *Nano Lett.* **2016**, *16*, 459.

[89] F. Makhlooghiazad, D. Gunzelmann, M. Hilder, D. R. MacFarlane, M. Armand, P. C. Howlett, M. Forsyth, *Adv. Energy Mater.* **2017**, *7*, 1601272.

[90] D. R. MacFarlane, M. Forsyth, P. C. Howlett, S. Kar, S. Passerini, J. M. Pringle, H. Ohno, M. Watanabe, F. Yan, W. Zheng, S. Zhang, J. Zhang, *Nat. Rev. Mater.* **2016**, *1*, 15005.

[91] I. Villaluenga, X. Bogle, S. Greenbaum, I. Gil de Muro, T. Rojo, M. Armand, *J. Mater. Chem. A* **2013**, *1*, 8348.

[92] L. M. Bronstein, R. L. Karlinsey, B. Stein, Z. Yi, J. Carini, J. W. Zwanziger, *Chem. Mater.* **2006**, *18*, 708.

[93] J. Christensen, P. Albertus, R. S. Sanchez-Carrera, T. Lohmann, B. Kozinsky, R. Liedtke, J. Ahmed, A. Kojic, *J. Electrochem. Soc.* **2012**, *159*, R1.

[94] Y. Wang, W. D. Richards, S. P. Ong, L. J. Miara, J. C. Kim, Y. Mo, G. Ceder, *Nat. Mater.* **2015**, *14*, 1026.

[95] A. Manthiram, X. Yu, S. Wang, *Nat. Rev. Mater.* **2017**, *2*, 16103.

[96] J. C. Bachman, S. Muy, A. Grimaud, H. H. Chang, N. Pour, S. F. Lux, O. Paschos, F. Maglia, S. Lupart, P. Lamp, L. Giordano, Y. Shao-Horn, *Chem. Rev.* **2016**, *116*, 140.

[97] J. B. Goodenough, H. Y. P. Hong, J. A. Kafalas, *Mater. Res. Bull.* **1976**, *11*, 203.

[98] H. Y. P. Hong, *Mater. Res. Bull.* **1976**, *11*, 173.

[99] Y. F. Y. Yao, J. T. Kummer, *J. Inorg. Nucl. Chem.* **1967**, *29*, 2453.

[100] B. Dunn, B. B. Schwarz, J. O. Thomas, P. E. D. Morgan, *Solid State Ionics* **1988**, *28–30*, 301.

[101] G. Yamaguchi, K. Suzuki, *Bull. Chem. Soc. Jpn.* **1968**, *41*, 93.

[102] S. Lee, S. Kim, M. Jang, S. Hwang, J. Haw, S. Lim, *J. Ceram. Process. Res.* **2010**, *11*, 86.

[103] A. P. De Kroon, G. W. Schafer, F. Aldinger, *Chem. Mater.* **1995**, *7*, 878.

[104] C. Chi, H. Katsui, T. Goto, *Ceram. Int.* **2017**, *43*, 1278.

[105] L. Viswanathan, Y. Ikuma, A.V. Virkar, *J. Mater. Sci.* **1983**, *18*, 109.

[106] G. Chen, J. Lu, L. Li, L. Chen, X. Jiang, *J. Alloys Compd.* **2016**, *673*, 295.

[107] X. Lu, G. Xia, J. P. Lemmon, Z. Yang, *J. Power Sources* **2010**, *195*, 2431.

[108] S. J. Shan, L. P. Yang, X. M. Liu, X. L. Wei, H. Yang, X. D. Shen, *J. Alloys Compd.* **2013**, *563*, 176.

[109] D. La Rosa, G. Monforte, C. D'Urso, V. Baglio, V. Antonucci, A. S. Arico, *ChemSusChem* **2010**, *3*, 1390.

[110] S.-T. Lee, D.-H. Lee, J.-S. Kim, S.-K. Lim, *Met. Mater. Int.* **2017**, *23*, 246.

[111] B. L. Tian, C. Chen, Y. R. Li, W. L. Zhang, L. X. Zhao, *Chin. Phys. B* **2012**, *21*, 126102.

[112] A. Mali, A. Petric, *J. Eur. Ceram. Soc.* **2012**, *32*, 1229.

[113] R. Subasri, T. Matews, O. M. Sreedharan, V. S. Raghunathan, *Solid State Ionics* **2003**, *158*, 199.

[114] G. Flor, A. Marini, V. Massarotti, M. Villa, *Solid State Ionics* **1981**, *2*, 195.

[115] M. Guin, F. Tietz, *J. Power Sources* **2015**, *273*, 1056.

[116] Q. Ma, M. Guin, S. Naqash, C.-L. Tsai, F. Tietz, O. Guillon, *Chem. Mater.* **2016**, *28*, 4821.

[117] F. G. Will, *J. Electrochem. Soc.* **1976**, *123*, 834.

[118] W. Bogusz, F. Krok, W. Jakubowski, *Solid State Ionics* **1983**, *9–10*, 803.

[119] Y. Ruan, S. Song, J. Liu, P. Liu, B. Cheng, X. Song, V. Battaglia, *Ceram. Int.* **2017**, *43*, 7810.

[120] F. Krok, D. Kony, J. R. Dygas, W. Jakubowski, W. Bogusz, *Solid State Ionics* **1989**, *36*, 251.

ADVANCED
SCIENCE NEWS

www.advancedsciencenews.com

ADVANCED
ENERGY
MATERIALS

www.advenergymat.de

[121] J. W. Fergus, *Solid State Ionics* **1989**, *36*, 251.

[122] R. O. Fuentes, F. Figueiredo, F. M. B. Marques, J. I. Franco, *Solid State Ionics* **2001**, *139*, 309.

[123] C. Cao, Z. Bin Li, X. L. Wang, X. B. Zhao, W. Q. Han, *Front. Energy Res.* **2014**, *2*, 1.

[124] M. Tatsumisago, M. Nagao, A. Hayashi, *J. Asian Ceram. Soc.* **2013**, *1*, 17.

[125] K. Noi, A. Hayashi, M. Tatsumisago, *J. Power Sources* **2014**, *269*, 260.

[126] A. Hayashi, K. Noi, A. Sakuda, M. Tatsumisago, *Nat. Commun.* **2012**, *3*, 856.

[127] A. Hayashi, K. Noi, N. Tanibata, M. Nagao, M. Tatsumisago, *J. Power Sources* **2014**, *258*, 420.

[128] M. Jansen, U. Henseler, *J. Solid State Chem.* **1992**, *99*, 110.

[129] N. J. J. de Klerk, M. Wagemaker, *Chem. Mater.* **2016**, *28*, 3122.

[130] N. Tanibata, K. Noi, A. Hayashi, M. Tatsumisago, *RSC Adv.* **2014**, *4*, 17120.

[131] I.-H. Chu, C. S. Kompella, H. Nguyen, Z. Zhu, S. Hy, Z. Deng, Y. S. Meng, S. P. Ong, *Sci. Rep.* **2016**, *6*, 33733.

[132] Z. Zhu, I.-H. Chu, Z. Deng, S. P. Ong, *Chem. Mater.* **2015**, *27*, 8318.

[133] H. Wang, Y. Chen, Z. D. Hood, G. Sahu, A. S. Pandian, J. K. Keum, K. An, C. Liang, *Angew. Chem., Int. Ed.* **2016**, *55*, 8551.

[134] Z. Yu, S.-L. Shang, J.-H. Seo, D. Wang, X. Luo, Q. Huang, S. Chen, J. Lu, X. Li, Z.-K. Liu, D. Wang, *Adv. Mater.* **2017**, *29*, 1605561.

[135] L. Zhang, K. Yang, J. L. Mi, L. Lu, L. R. Zhao, L. M. Wang, Y. M. Li, H. Zeng, *Adv. Energy Mater.* **2015**, *5*, 1501294.

[136] A. Banerjee, K. H. Park, J. W. Heo, Y. J. Nam, C. K. Moon, S. M. Oh, S.-T. Hong, Y. S. Jung, *Angew. Chem., Int. Ed.* **2016**, *55*, 9634.

[137] S.-H. Bo, Y. Wang, G. Ceder, *J. Mater. Chem. A* **2016**, *4*, 9044.

[138] G. Sahu, Z. Lin, J. C. Li, Z. C. Liu, N. Dudney, C. D. Liang, *Energy Environ. Sci.* **2014**, *7*, 1053.

[139] S. Nishimura, N. Tanibata, A. Hayashi, M. Tatsumisago, A. Yamada, *J. Mater. Chem. A* **2017**, *5*, 25025.

[140] W. D. Richards, T. Tsujimura, L. J. Miara, Y. Wang, J. C. Kim, S. P. Ong, I. Uechi, N. Suzuki, G. Ceder, *Nat. Commun.* **2016**, *7*, 11009.

[141] Y. Wang, W. D. Richards, S.-H. Bo, L. J. Miara, G. Ceder, *Chem. Mater.* **2017**, *29*, 7475.

[142] L. Duchene, R.-S. Kuhnel, D. Rentsch, A. Remhof, H. Hagemann, C. Battaglia, *Chem. Commun.* **2017**, *53*, 4195.

[143] B. R. S. Hansen, M. Paskevicius, M. Jørgensen, T. R. Jensen, *Chem. Mater.* **2017**, *29*, 3423.

[144] Y. Sadikin, P. Schouwink, M. Brighi, Z. Łodziana, R. Cerny, *Inorg. Chem.* **2017**, *56*, 5006.

[145] T. J. Udovic, M. Matsuo, W. S. Tang, H. Wu, V. Stavila, A. V. Soloninin, R. V. Skoryunov, O. A. Babanova, A. V. Skripov, J. J. Rush, *Adv. Mater.* **2014**, *26*, 7622.

[146] W. S. Tang, A. Unemoto, W. Zhou, V. Stavila, M. Matsuo, H. Wu, S.-I. Orimo, T. J. Udovic, *Energy Environ. Sci.* **2015**, *8*, 3637.

[147] J. Zhu, Y. Wang, S. Li, J. W. Howard, J. Neuefeind, Y. Ren, H. Wang, C. Liang, W. Yang, R. Zou, C. Jin, Y. Zhao, *Inorg. Chem.* **2016**, *55*, 5993.

[148] Y. Wang, Q. Wang, Z. Liu, Z. Zhou, S. Li, J. Zhu, R. Zou, Y. Wang, J. Lin, Y. Zhao, *J. Power Sources* **2015**, *293*, 735.

[149] R. D. Shannon, B. E. Taylor, T. E. Gier, H.-Y. Chen, T. Berzins, *Inorg. Chem.* **1978**, *17*, 958.

[150] H. Y.-P. Hong, J. A. Kafalas, M. Bayard, *Mater. Res. Bull.* **1978**, *13*, 757.

[151] H. Muramatsu, A. Hayashi, T. Ohtomo, S. Hama, M. Tatsumisago, *Solid State Ionics* **2011**, *182*, 116.

[152] M. W. Breiter, G. C. Farrington, W. L. Roth, J. L. Duffy, *Mater. Res. Bull.* **1977**, *12*, 895.

[153] J. L. Briant, G. C. Farrington, *J. Electrochem. Soc.* **1981**, *128*. 1830.

[154] G. C. Farrington, J. L. Briant, *Mater. Res. Bull.* **1978**, *13*, 763.

[155] Y. C. Jung, S. M. Lee, J.-H. Choi, S. S. Jang, D. W. Kim, *J. Electrochem. Soc.* **2015**, *162*, A704.

[156] T. Inada, K. Takada, A. Kajiyama, M. Kouguchi, H. Sasaki, S. Kondo, M. Watanabe, M. Murayama, R. Kanno, *Solid State Ionics* **2003**, *158*, 275.

[157] Z. Zhang, Q. Zhang, C. Ren, F. Luo, Q. Ma, Y.-S. Hu, Z. Zhou, H. Li, X. Huang, L. Chen, *J. Mater. Chem. A* **2016**, *4*, 15823.

[158] L. Liu, X. Qi, Q. Ma, X. Rong, Y.-S. Hu, Z. Zhou, H. Li, X. Huang, L. Chen, *ACS Appl. Mater. Interfaces* **2016**, *8*, 32631.

[159] K. Park, J. H. Cho, J. H. Jang, B. C. Yu, A. T. De la Hoz, K. M. Miller, C. J. Ellison, J. B. Goodenough, *Energy Environ. Sci.* **2015**, *8*, 2389.

[160] H. Gao, W. Zhou, K. Park, J. B. Goodenough, *Adv. Energy Mater.* **2016**, *6*, 1600467.

[161] W. Zhou, S. Wang, Y. Li, S. Xin, A. Manthiram, J. B. Goodenough, *J. Am. Chem. Soc.* **2016**, *138*, 9385.

[162] S. Yubuchi, A. Hayashi, M. Tatsumisago, *Chem. Lett.* **2015**, *44*, 884.

[163] R. Knödler, *J. Appl. Electrochem.* **1984**, *14*, 39.

[164] I. Kim, J.-Y. Park, C. H. Kim, J.-W. Park, J.-P. Ahn, J.-H. Ahn, K.-W. Kim, H.-J. Ahn, *J. Power Sources* **2016**, *301*, 332.

[165] X. Yu, A. Manthiram, *Adv. Energy Mater.* **2015**, *5*. 1500350.

[166] X. Yu, A. Manthiram, *J. Phys. Chem. Lett.* **2014**, *5*, 1943.

[167] T. Wei, Y. Gong, X. Zhao, K. Huang, *Adv. Funct. Mater.* **2014**, *24*, 5380.

[168] F. Lalère, J. B. Leriche, M. Courty, S. Boulineau, V. Viallet, C. Masquelier, V. Seznec, *J. Power Sources* **2014**, *247*, 975.

[169] T. Wei, Y. Gong, X. Zhao, K. Huang, *Adv. Funct. Mater.* **2014**, *24*, 5380.

[170] W. Zhou, Y. Li, S. Xin, J. B. Goodenough, *ACS Cent. Sci.* **2017**, *3*, 52.

[171] R. P. Rao, H. Chen, L. L. Wong, S. Adams, *J. Mater. Chem. A* **2017**, *5*, 3377.

[172] J. Yue, F. Han, X. Fan, X. Zhu, Z. Ma, J. Yang, C. Wang, *ACS Nano* **2017**, *11*, 4885.

[173] S. Wenzel, T. Leichtweiss, D. A. Weber, J. Sann, W. G. Zeier, J. Janek, *ACS Appl. Mater. Interfaces* **2016**, *8*, 28216.

[174] A. Wang, X. Hu, H. Tang, C. Zhang, S. Liu, Y.-W. Yang, Q.-H. Yang, J. Luo, *Int. Ed.* **2017**, *129*, 1.

[175] W. Luo, Y. Zhang, S. Xu, J. Dai, E. Hitz, Y. Li, C. Yang, C. Chen, B. Liu, L. Hu, *Nano Lett.* **2017**, *17*, 3792.

[176] Y.-J. Kim, H. Lee, H. Noh, J. Lee, S. Kim, M.-H. Ryou, Y. M. Lee, H.-T. Kim, *ACS Appl. Mater. Interfaces* **2017**, *9*, 6000.

[177] C. Zhao, Q. Wang, Y. Lu, Y.-S. Hu, B. Li, L. Chen, *J. Phys. D: Appl. Phys.* **2017**, *50*, 183001.

[178] Y. Li, Y. Lu, C. Zhao, Y.-S. Hu, M.-M. Titirici, H. Li, X. Huang, L. Chen, *Energy Storage Mater.* **2017**, *7*, 130.

1703012 (20 of 20)